TECHNICAL NOTES

NATIONAL ADVISORY COMMITTEE FOR AERONAUTICS

No. 777

INTERNAL-FLOW SYSTEMS FOR AIRCRAFT

By F. M. Rogallo
Langley Memorial Aeronautical Laboratory

Washington
October 1940

NATIONAL ADVISORY COMMITTEE FOR AERONAUTICS

TECHNICAL NOTE NO. 777

INTERNAL-FLOW SYSTEMS FOR AIRCRAFT

By F. M. Rogallo

SUMMARY

An investigation has been made to determine efficient arrangements for an internal-flow system of an aircraft when such a system operates by itself or in combination with other flow systems. The investigation included a theoretical treatment of the problem and tests in the NACA 5-foot vertical wind tunnel of inlet and outlet openings in a flat plate and in a wing.

When an internal-flow system tends to decrease the final velocity of its wake, the results showed that it should be arranged in series with the propulsive system; the inlet opening should be located at a forward stagnation point; and the outlet opening should be so shaped and located as to recover the kinetic energy of the jet without increasing the drag of other portions of the aircraft. When an internal-flow system tends to increase the final velocity of its wake, as does a propeller, location of the inlet opening in the boundary layer or in the wake of the wing or the fuselage may be desirable.

INTRODUCTION

The ideal aerodynamic characteristics of aircraft-radiator installations have been determined by a consideration of the radiator as an actuator disk operating on a perfect fluid. In the treatment by Meredith (reference 1) the cooling system was assumed to be operating in previously undisturbed fluid. Because it is often necessary and may sometimes be aerodynamically advantageous to deviate from that condition in actual installations, an extension of the previous theory was considered desirable.

In the present investigation, simple equations are derived for the calculation of the drag, the pressure characteristics, and the efficiency of internal-flow systems either isolated or in combination with propellers,

wings, or fuselages. These equations cover the range of outlet velocities from zero to above that of the free stream.

Experimental data obtained in a 5-foot vertical wind tunnel are presented to verify the theory. The application of the results to the design of aircraft is discussed. The investigation was completed early in 1938

SYMBOLS

A	area
c	chord
C_D	drag coefficient (D/qA)
C_{PL}	power-loss coefficient
D	drag
H	total pressure
ΔH	total-pressure loss
$K_{i,o}$	velocity ratio $(V_{i,o}/V)$
p	static pressure relative to that of the free stream
Q	volume rate of flow
q	dynamic pressure
V	velocity of the free stream
$V_{i,o}$	hypothetical inlet or outlet velocity corresponding to total pressure
V'	local velocity
η_p	pump efficiency
η	propulsive efficiency
ρ	mass density
σ	density ratio relative to the free stream

Subscripts:

d duct

r resistance

i inlet

o outlet

i,o inlet or outlet

THEORY

Isolated Systems

If the radiators of figure 1 are considered to be actuator disks operating in a perfect fluid, their ideal characteristics may be written as follows:

Drag $$D = Q\rho \quad (V - V_o) \tag{1}$$

Drag power $$DV = 2Qq \quad (1 - K_o) \tag{2}$$

Total-pressure loss $$\Delta H = q \quad (1 - K_o^2) \tag{3}$$

Pump efficiency $$\eta_p = \frac{\Delta HQ}{VD} = \frac{1 + K_o}{2} \tag{4}$$

The pump efficiency may also be written

$$\eta_p = \frac{1 + \sqrt{1 - \Delta H/q}}{2} \tag{5}$$

In equations (4) and (5), which are the equivalent of equations (3) and (11), respectively, of reference 1, it is assumed that the internal power ΔHQ is usefully employed.

If a fan is included in the system in series with the radiator, equations (1) to (5) will be applicable as long as the over-all ΔH is positive; that is, as long as $V_o < V$. When ΔH becomes negative and $V_o > V$, the system will provide propulsion and equations (4) and (5) may

be replaced by their reciprocals, expressions for propulsive efficiency,

$$\eta = \frac{VD}{\Delta HQ} = \frac{2}{1 + K_o} \tag{6}$$

and

$$\eta = \frac{2}{1 + \sqrt{1 - \Delta H/q}} \tag{7}$$

Equations (6) and (7) are the equivalent of those given in reference 2 for isolated propellers.

Systems Operating in Slipstream or Wake

When an internal-flow system operates in the propeller slipstream or in the boundary layer or the wake of an aerodynamic body such as a wing or fuselage, the inlet velocity may differ from that of an isolated system. (See fig. 2.) The ideal characteristics of the system may be written as follows:

$$D = Q\rho\ (V_i - V_o) \tag{8}$$

$$DV = 2Qq\ (K_i - K_o) \tag{9}$$

$$\Delta H = q\ (K_i^2 - K_o^2) \tag{10}$$

$$\eta_p = \frac{\Delta HQ}{DV} = \frac{K_i + K_o}{2} = \frac{K_i + \sqrt{K_i^2 - \Delta H/q}}{2} \tag{11}$$

$$\eta = \frac{DV}{\Delta HQ} = \frac{2}{K_i + K_o} = \frac{2}{K_i + \sqrt{K_i^2 - \Delta H/q}} \tag{12}$$

Equations (11) and (12) are plotted in figure 3. The pump efficiency is shown to increase with K_i because the power usefully consumed ΔHQ increases faster than the drag power DV. This principle implies that an internal-flow system with an inlet opening in the propeller slipstream may have a higher pump efficiency than a system operating in the free stream. The slipstream inlet opening therefore offers not only higher available pressures

on the ground and in climb but a small reduction in the drag of the internal-flow system for a given internal power at cruising and top speeds.

The propulsive efficiency η is an inverse function of K_i. Systems including blowers should therefore have their highest efficiencies when operating in the boundary layer or in the wake of wings, fuselages, or other bodies that have decreased the total pressure of the field. This principle explains the commonly known fact that a propeller operating in the wake of a body may be more efficient than a propeller operating in the free stream.

In many internal-flow systems neither pump efficiency nor propulsive efficiency is of importance, the object being to obtain a given internal flow of air with the least possible loss or waste of power,

$$DV - \Delta HQ \tag{13}$$

A criterion of merit for such a system may be defined as

$$\text{Power-loss coefficient} \quad C_{PL} = \frac{DV - \Delta HQ}{qQ} \tag{14}$$

If equations (9) and (10) are substituted in equation (14) and the result is simplified,

$$C_{PL} = (K_o - 1)^2 - (K_i - 1)^2 \tag{15}$$

or

$$C_{PL} = 2\left(K_i - \sqrt{K_i^2 - \Delta H/q}\right) - \Delta H/q \tag{16}$$

Equations (15) and (16) are plotted in figure 4. It may be seen that minimum C_{PL} occurs when K_o equals unity and when K_i is at a minimum for systems giving thrust or at a maximum for systems experiencing drag.

Although the pump efficiency, the propulsive efficiency, and the power-loss coefficient each has its own particular field of usefulness, the conversion from one to the other by means of the following equations may be desirable.

$$\eta = 1 + \frac{C_{PL}}{\Delta H/q} \tag{17}$$

$$\eta_p = \left(1 + \frac{C_{PL}}{\Delta H/q}\right)^{-1} \tag{18}$$

Individual Openings

It is often convenient to consider the various parts of an internal-flow system as well as the complete system. When openings are individually considered, it may be assumed for convenience that fluid entering the inlet opening remains within the aircraft or that fluid previously within the aircraft is ejected through the outlet opening. In either case the mass of the moving system (the aircraft) would be changed at the rate $Q\rho$, which represents a rate of change of kinetic energy qQ. The ideal characteristics of inlet and outlet openings may be written as follows:

$$D_i = Q\rho V_i \tag{19}$$

$$D_o = -Q\rho V_o \tag{20}$$

$$H_i = qK_i^2 \tag{21}$$

$$H_o = qK_o^2 \tag{22}$$

$$C_{PL_i} = \frac{VD_i - (H_iQ + qQ)}{qQ} = -(K_i - 1)^2 \tag{23}$$

$$C_{PL_o} = \frac{VD_o + (H_oQ + qQ)}{qQ} = (K_o - 1)^2 \tag{24}$$

$$\eta_{p_i} = \frac{H_iQ + qQ}{VD_i} = \frac{K_i^2 + 1}{2K_i} \tag{25}$$

$$\eta_o = \frac{-VD_o}{H_oQ + qQ} = \frac{2K_o}{K_o^2 + 1} \tag{26}$$

In the foregoing equations $(H_iQ + qQ)$ is the available power and $(H_oQ + qQ)$ is the expended power of the internal flow at the inlet and the outlet, respectively.

Effect of Heat Exchange and Combustion

In the foregoing ideal-fluid theory, the density ρ of the fluid entering or leaving internal-flow systems was assumed to be the same as that of the free stream and the volume rates of flow Q through the two openings of complete systems were assumed to be equal. Thus Q and ρ were used without subscripts. When variations of Q and ρ are considered, subscripts are required for identification; the equations of drag and pressure, (19) to (22), then become

$$D_i = \sigma_i Q_i \rho V_i \tag{27}$$

$$D_o = - \sigma_o Q_o \rho V_o \tag{28}$$

$$H_i = \sigma_i q K_i^2 \tag{29}$$

$$H_o = \sigma_o q K_o^2 \tag{30}$$

Any of the other equations (1) to (26) may be readily altered to include variations of σ and Q.

The formulas for power-loss coefficients and efficiencies as functions of the velocity ratios are unaffected by variations of density. The numerical values for any particular case, however, are dependent upon the addition or the loss of heat just as they are dependent upon the addition or the loss of pressure energy within the system. Although the system may allow the recovery of heat energy, it is not credited with that recovery in the criterions of merit. Instead, the heat energy is treated in the same manner as the pressure energy supplied by a blower. The heat energy recovered may be calculated (see references 1 and 3) for any particular case, however, and can be either deducted from the power loss or added to the useful work of the internal-flow system to obtain over-all criterions.

WIND-TUNNEL ARRANGEMENT

The test set-up for this investigation is shown in figure 5. The 5-foot vertical wind tunnel (see reference 4) was modified by the installation of a flat plywood panel parallel to and 18 inches from the center line of the orig-

inal test section. This panel was faired into the entrance cone in such a manner as to provide acceptable flow conditions in the modified test section.

The internal-flow system comprised a floating chamber having internal dimensions of 16 by 16 by 20 inches, a variable-speed centrifugal blower, and a calibrated flowmeter. This system allowed close regulation and accurate metering of the flow over a wide range in both directions.

The balance system was composed of a ball-bearing jointed parallelogram restrained in the drag direction by an automatic electric balance as shown in figure 5. The duct, which formed two sides of the parallelogram, was flexibly coupled at the pivots in such a way as to eliminate the necessity for drag corrections due to static pressure in the system. That such corrections were negligible was experimentally verified. It was found, however, that flow through the duct had a small but measurable effect upon the drag readings. Suitable corrections were experimentally determined.

MODELS

A wide range of opening shapes was tested on a flat plate and a few were tested in a small wing of NACA 0018 airfoil section. A dimensioned drawing of each opening is included in the figure that presents the principal aerodynamic characteristics of the particular opening. All the openings tested on the flat plates were mounted on 1/16-inch steel plates, which fitted into the end of the floating chamber, as shown in figure 5. The openings through the plate were located symmetrically with respect to the horizontal and the vertical center lines of the plate except for recessed openings with rectangular ducts. These ducts were displaced 5 inches vertically off center.

The wing in which openings were tested had a chord of 3 feet and a span of 3 feet exclusive of the faired tip. When the wing was mounted in the tunnel, a steel plate at its end was fastened to the floating chamber (fig. 5) as though the complete wing were an opening being tested on the flat mounting plate.

Two ribs divided the interior of the wing into three nearly equal compartments, the central one having a clear width of 12 inches. Figure 6, a cross section of the cen-

tral wing compartment, shows the arrangement of external openings, rib openings, leading-edge duct, resistance, and static-pressure stations. All openings were located and adjusted symmetrically with respect to the chord line, and the wing was set at zero angle of attack for all tests. The inboard and the outboard wing compartments were interconnected by the leading-edge duct, and the flow path into these compartments from the central one was controlled by corks that fitted snugly into the rib openings. Thus, all the air that flowed through any set of external openings was made to pass through the resistance before escaping from the central wing compartment.

TEST METHODS

Flat Plate

All of the openings in the flat plate were tested at an air-stream velocity of 40 miles per hour and some of the openings were also tested at 80 miles per hour. Boundary-layer surveys on a plate without openings were made at the two stream velocities. Velocity profiles at three stations along the vertical center line of the plate are shown in figure 7(a). Profiles at 6 inches on either side of the vertical center line were not significantly different from those shown.

During the tests of the openings the stream velocity was held constant, and the drag and the static pressure were recorded at several velocities of flow through the openings. It was generally possible to obtain reasonably steady conditions during observations; but some inlet openings apparently induced pulsations that adversely affected their drag and pressure characteristics, particularly at low values of the flow coefficient. These pulsations occurred even when the blower was inoperative and the flowmeter orifice was closed but were nearly eliminated by the partial closing of the butterfly damper shown in figure 5. Their effect upon the test results was therefore thought to be small, but the possibility of the occurrence of pulsations under actual flight conditions and of resulting significant drag increases should not be overlooked.

Many of the openings were fitted with short lengths of duct that extended into the floating chamber, as shown in figure 5. Under some inlet conditions, relatively large

ststic-pressure gradients were observed along the ducts, as shown in figure 8. These gradients, which may be expected downstream of any sharp bend (see reference 5), showed that approximately four pipe diameters inside the opening were required for maximum static-pressure recovery. Whenever practicable, the pressure tap was located in this region of maximum static pressure during routine tests of inlet openings with ducts.

Owing to the use of a bellmouth at the end of the duct inside the floating chamber, as shown in figure 5, the static-pressure gradients in the ducts of outlet openings were relatively small, approximately the same as those for straight-pipe loss. In routine tests of outlet openings with ducts, the pressure tap was generally located within one duct diameter of the outlet opening in order to eliminate the pressure loss due to straight duct friction from the pressure measurements.

Many of the openings were not fitted with ducts; the air flowed directly into or out of the floating chamber and the static pressure was determined at the center of the top face of the floating chamber.

Wing

The inlet and the outlet openings in the NACA 0018 wing were tested in much the same manner as were the openings in the flat plate. Openings were located symmetrically about the chord line at the leading edge, at 0.175c, and at 0.800c. The local velocities outside the boundary layer at these locations were 0.00V, 1.29V, and 1.02V, respectively, V being 80 miles per hour. The effect of the boundary layer on the inlet-velocity ratio of openings at the nose and at 0.175c was negligible. The boundary-layer profiles at 0.800c, shown in figure 7(b), were determined with the adjustable-flap openings closed and sealed at 0.175c and 0.800c. The drag of the wing in this condition was also determined and was considered to be the tare drag for the adjustable-flap openings. The tare drag for the fixed openings was the drag of the wing with all openings replaced by smooth plates that conformed to the wing contour; it was slightly lower than the tare drag for the adjustable openings.

When either inlet or outlet openings were tested, the procedure was the same as for flat-plate tests. In all tests, the static pressures observed were those at stations

0 or -0. (See fig. 6.) Consequently, the characteristics presented include duct losses.

REDUCTION OF DATA

The data have been reduced to dimensionless coefficients. The flow coefficient Q/AV is the ratio of the average velocity through the area A to the velocity of the free stream, where A is the minimum cross-sectional area of the opening as determined from measurements of the model as tested. The drag coefficient ($C_{D_{i,o}} = D_{i,o}/qA$) is based on the same area of opening as the flow coefficient; and $D_{i,o}$ is the total drag minus the drag of the 20-inch-square floating plate or of the wing without openings.

The static-pressure coefficient p/q is the ratio of static pressure at the pressure tap to the dynamic pressure in the free stream. The coefficient of total pressure in the ducts was calculated from the static-pressure and the flow coefficients and was based on the assumption of uniform duct velocity.

In the presentation of the data of individual openings, the power-loss coefficient $C_{PL_{i,o}}$ was considered the best criterion of merit and was computed from the drag, the flow, and the total-pressure coefficients by means of the following equations:

$$C_{PL_i} = \frac{D_i/qA}{Q/AV} + (H_i/q + 1) \tag{31}$$

$$C_{PL_o} = \frac{D_o/qA}{Q/AV} + (H_o/q + 1) \tag{32}$$

RESULTS AND DISCUSSION

Inlet Openings

The ideal characteristics of inlet openings at several inlet-velocity ratios are shown in figure 9. The drag and

the pressure coefficients were plotted from the following equations:

$$C_{D_i} = \frac{D_i}{qA} = 2 \frac{Q}{AV} K_i \tag{33}$$

$$\frac{p}{q} = K_i^2 - \left(\frac{A}{A_d}\right)^2 \left(\frac{Q}{AV}\right)^2 \tag{34}$$

where (A/A_d) was assumed to be unity. These equations were derived from equations (19) and (21).

Circular holes in a flat plate.- The inlet characteristics of circular holes in a flat plate are shown in figure 10. The inlet-velocity ratio K_i may be roughly estimated from the boundary-layer velocity distributions of figure 7(a). At low values of Q/AV, the inflow was principally from the boundary layer where K_i was low; hence, the slope of the drag curve was low. As Q/AV was increased, K_i was increased and the slope of the drag curve increased, as would be expected from the relationship of equation (33). Because these openings had very little external drag, their drag curves lie completely below the drag curve for an ideal opening in the free stream, where $K_i = 1.0$. (See fig. 9.)

The experimental drag curves for the two opening diameters and air speeds are not coincident but diverge in a consistent manner. The curves for 40 miles per hour lie above the curves for 80 miles per hour because the boundary layer was thicker at 80 miles per hour, as shown in figure 7(a). The drag curves for the 3-inch holes, moreover, lie above the corresponding curves for the 2-inch holes because the ratio of opening width to boundary-layer thickness was greater for the 3-inch holes. Because inlet characteristics are largely dependent upon the total-pressure gradient ahead of the opening, the data presented in this report are not directly applicable where the external boundary-layer conditions differ from those of the test set-up.

The pressure curves indicate that these openings did not tend to scoop air from the passing stream; inflow was maintained only when the internal static pressure was decreased below that outside the opening. Openings of this

type should not be used as inlet openings for internal-flow systems because of their extremely poor pressure characteristics; the high values of C_{PL_i} in figure 10 are due almost entirely to pressure losses. Because of the existence of static-pressure gradients on aerodynamic bodies, however, small holes in the surfaces of aircraft may result in internal flow where none is desired. The drag accompanying such flow may be estimated from the results given in figure 10 and in the following figures.

Adjustable-flap openings in a flat plate.- The inlet characteristics of adjustable-flap openings in a flat plate are shown in figures 11 and 12. These openings were made in 1/16-inch steel plate having plane surfaces and square edges. Characteristics of the internal flap deflected 45° were roughly similar to those of the circular hole because the flow was unable to follow the contour of the opening. As the flap angle was decreased, the flow tended to follow the opening contour more closely, thereby causing a scooping action that decreased the pressure loss over the complete flow range but increased the external drag, that is, increased the difference between total and ideal drag, at and near zero flow coefficient. Increasing the deflection of the external flap (fig. 12) increased the static-pressure, the drag, and the power-loss coefficients. Adjustable-flap openings, like the circular holes, had high internal losses.

Flush openings with circular ducts in a flat plate.- The inlet characteristics of flush openings with circular ducts at three angles relative to a flat plate parallel with the stream direction are shown in figure 13. The drag characteristics are very much like those of figure 10, but the internal-pressure losses, and consequently the power-loss coefficients, were considerably lower. As would be expected, the internal loss decreased as the angle between the duct and the plate was decreased. Some of the discrepancy between the curves of power-loss coefficient for model 3P30-90 at 40 and 80 miles per hour may have been due to experimental error, although the difference in boundary-layer thickness would account for a part of it. This model was one of the first to be tested; only half the usual number of points were taken, and one of these points is noticeably below the curve drawn.

Circular pipes protruding from a flat plate.- The inlet characteristics of circular pipes protruding above the

surface of a flat plate are shown in figures 14 and 15. Model variations included height of protrusion, end treatment, and rear fairing. The models were made of 3-inch outside-diameter seamless-steel tubing of about 0.080-inch wall thickness. All of these models had a large external drag at low values of the flow coefficient, but the drag of the faired models was near the ideal drag at flow coefficients near unity. The pressure characteristics were greatly affected by end treatment, relatively little by height above the surface, and negligibly by rear fairing. These openings were tested because of their extreme simplicity of design and construction. They would not be used where aerodynamic efficiency is the chief consideration.

Conventional scoops on a flat plate.- The inlet characteristics of external scoops on a flat plate are shown in figures 16 to 18. The models of this group, formed from 1/32-inch sheet copper, were, in general, similar to openings found on production airplanes at the time the investigation was made. Figure 16 shows the effects of variations in the shape of the scoop entrance, the rear fairing, and the duct angle on the characteristics of scoops with circular ducts. Necking down the scoop entrance and adding a rear fairing were found to decrease the power loss. Reduction of the duct angle to 45° reduced the pressure loss as expected but appeared to increase the drag somewhat; this drag increase has not been accounted for.

Figures 17 and 18 show the effects of variations in scoop shape upon the characteristics of scoops without ducts. Model 13P925 of figure 17 appeared to be the best of this group on a power-loss basis, but model 15P-G of figure 18 gave the highest pressure up to $Q/AV = 0.5$. The guide vanes in model 15P-G, as in all the models tested with vanes, were made of thin sheet brass and shaped as recommended in reference 5. For the high scoop, the static-pressure coefficient near zero Q/AV was nearly unity; that for the half-round opening was only about 0.6. This difference was due to the effect of the external boundary layer.

Recessed openings in a flat plate.- The inlet characteristics of recessed openings with ducts in a flat plate are presented in figures 19 and 20. The models, including ducts, were of rectangular cross section and practically all of the surfaces were plane. Model variations included

recess angle, cover-plate length and projection, and bend treatment. The installation of guide vanes was again found to reduce the pressure loss, as expected from the results of reference 5. The external drag of all of the openings was relatively small in the region of minimum power loss, but the external drag of the protruding devices was relatively large at and near zero flow coefficient. Boundary-layer conditions are thought to have a considerable influence on the characteristics of this type of inlet opening.

Wing openings.- The inlet characteristics of openings in the NACA 0018 wing are presented in figures 21, 22, and 23. In general, the adjustable-flap openings (figs. 21 and 22), particularly those at 0.175c, had a high external drag. The fixed openings, both in the leading edge and at 0.800c (fig. 23), had relatively small external drag. In all cases, the external drag decreased with increasing flow coefficient. The total drag of the nose openings and, to a lesser extent, the drag of the internal-flap openings at 0.175c was less than the ideal drag at flow coefficients near unity. These results may have been due to the reduction of velocity over the outside surface of the wing, which naturally accompanied flow into the wing near its leading edge; that is, the effective thickness of the wing was reduced. It will be noted that the drag curves for openings WRIA and WRIB (fig. 23) are virtually the same in spite of the fact that these openings face in opposite directions.

The observed pressure characteristics are of small practical value because no attempt was made to reduce the duct losses. In spite of this fact, the minimum power-loss coefficient of model WRIB (fig. 23) was less than 0.3. It is thought that the power-loss coefficient of this type of opening will be negative in some installations, as indicated by the theory.

The observed minimum power-loss coefficient of model WNI (fig. 23) was slightly less than 0.4, although the theoretical value was zero at all flow coefficients. The observed power loss was the result of external drag, which has been discussed, and pressure loss, which was largely due to the abrupt expansion of the duct at 0.128c. The power-loss coefficient ahead of this expansion was computed from the experimental data of figures 6 and 23; it is represented by the solid curve without experimental points in figure 23. This curve shows that the power-loss coeffi-

cient of these openings, not including the sudden expansion, was practically equal to the ideal value, zero, at flow coefficients above 0.5. The close agreement between experiment and theory for the special case of K_i equals unity indicates that this type of opening, when placed in the propeller slipstream where K_i exceeds unity, may have an actual power-loss coefficient of slightly less than zero.

Outlet Openings

The ideal characteristics of an outlet opening in a flat plate are shown in figure 24. The coefficients of drag and total pressure were plotted from the following equations:

$$C_{D_o} = \frac{D_o}{qA} = -2\frac{Q}{AV}K_o \tag{35}$$

$$\frac{H_o}{q} = K_o^2 \tag{36}$$

where K_o was assumed equal to Q/AV. These equations were derived from equations (20) and (22).

Circular hole in a flat plate.- The outlet characteristics of a circular hole in a flat plate are shown in figure 25. The thrust of this opening is almost zero at all flow coefficients because the jet is not directed downstream. The total energy of the jet is therefore wasted, and the power-loss coefficient is approximately equal to $(H_o/q + 1)$, as can be deduced from equation (32).

Adjustable-flap openings in a flat plate.- The outlet characteristics of adjustable-flap openings in a flat plate are shown in figures 26 to 28. Many variations of opening shape were tested but the single internal flap, as shown in figure 26, appeared to be about as efficient as any in this group. The experimental power-loss coefficients were below the theoretical (see fig. 24) up to pressure coefficients of about 0.5 and above the theoretical at higher pressure coefficients. The variation of skin friction on the plate behind the opening would tend to increase the drag with the flow coefficient, and the reduced velocities near the surface at low flow coefficients would be expected to give apparent power-loss coefficients below the ideal for openings of this type on a flat plate.

Models that projected above the surface of the plane had high drag coefficients at low flow coefficients but all models that deflected the air downstream gave thrust at high jet velocities. The drag coefficient of model 7S+20+20 (fig. 28), however, increased with flow coefficient. A comparison of the characteristics of this model with those of a flush opening (fig. 25) shows that a discharge or a leakage from a raised surface or a solid body may be many times as costly as from a flat plate.

Flush openings with circular ducts in a flat plate.- The outlet characteristics of flush openings with circular ducts at three angles with respect to a flat plate parallel with the free-stream direction are presented in figure 29. The magnitude of the thrust exerted by the jet from the 90° duct may be surprising, especially in view of the relatively small thrusts obtained from the openings in thin plate. (See fig. 25.) The close agreement between the characteristics of this opening at 40 and at 80 miles per hour is also noteworthy. The thrust of the 90° duct, though of academic interest, is of little practical importance in view of the very much greater thrusts that may be obtained by tilting the duct so as to give the jet a relatively large component in the direction of the external stream. The thrust of the 45° duct (fig. 29) is more than 80 percent of that indicated by equation (35) over most of its flow range.

In the construction of the total-pressure curve of figure 24, the static pressure at the opening was assumed to be the same as that of the free stream. The static-pressure curves of figure 29 show this assumption to be accurate at very small flow coefficients at all duct angles tested and to be fairly accurate over the complete flow range at the most efficient duct angle tested, 45°. The variation of the discrepancy indicates that it decreases with duct angle and is therefore of little importance for efficient outlets, that is, for outlets having duct angles of considerably less than 45°.

Circular pipes protruding from a flat plate.- The outlet characteristics of circular pipes protruding above the surface of a flat plate are shown in figures 30, 31, and 32. These openings were relatively inefficient, as was expected. They were tested because of their simplicity of design and construction and because the group included many arrangements commonly used as engine exhaust openings.

Straight pipes (figs. 30 and 31) had no bend loss and some aspirator effect but failed to utilize the kinetic energy of the air in the jet. Pipes with 90° elbows, on the other hand, derived thrust from the jet but at the expense of back pressure due to bend loss. The external drag of all the openings was rather high, especially of the openings without fairings and of those projecting farthest above the surface.

Conventional hoods on a flat plate.- The outlet characteristics of conventional hoods on a flat plate are shown in figures 33, 34, and 35. The characteristics of the flush-opening duct at 45° and 90° with the plate, as given in figure 29, are repeated in figure 33 for comparison with the characteristics of the same ducts with a conventional hood over the opening. The hood was found to be of considerable benefit to the 90° duct but of doubtful benefit to the 45° duct over most of the flow range. Constriction of flow at the hood opening by means of the faired block (see fig. 33) was found to be detrimental in the lower portion of the flow range and beneficial in the upper portion, the flow coefficient in all cases being based upon the minimum area of opening. Such a restriction in an opening with a given volume rate of flow or duct velocity would increase both the thrust and the back pressure.

Figure 34 shows that the drag of a hood at zero flow coefficient or of a blunt-end body, made by cutting off successive portions of a streamline form, was nearly proportional to the area of the cut surface. For a conventional hood outlet, moreover, the greater the portion of the basic streamline form retained, the smaller was the minimum power loss within the test range. Hood H of figure 34 was the same as the hood shown in figure 33.

Figure 35 shows that a high, thin hood was better with the guide vanes and worse without them than the conventional hood of figure 34 when discharging at its maximum cross section. None of these hoods, however, was as efficient as the elongated hoods of figure 34; even the elongated hoods were less efficient than some of the adjustable-flap outlets previously discussed.

Recessed openings in a flat plate.- The outlet characteristics of recessed openings with ducts in a flat plate are shown in figures 36 and 37. Guide vanes were again shown to be of considerable value, but the other variations

tested had little effect upon the minimum value of C_{PL_o}. These outlet openings had the lowest C_{PL_o} of any tested with ducts, although the flush opening shown in figure 29 would probably have had lower C_{PL_o} at duct angles below 45°. They were nearly as efficient as the best adjustable-flap openings tested. Comparisons between ducted and unducted openings, however, are of little value. Openings without ducts were expected to appear more efficient than openings with ducts because the conversion from static-pressure power into thrust power can be made more efficiently than the conversion from dynamic-pressure power, especially when the ducts approach the openings in a direction normal to that of the free stream, thereby necessitating bend losses in addition to straight duct losses.

The experimental characteristics shown in figures 36 and 37 may be roughly compared with the theoretical characteristics of figure 24. The experimental thrusts, particularly at high rates of flow, were somewhat greater than the theoretical, probably because the jet velocity was not uniform across the opening. Any departure from uniformity results in an increase of the jet momentum and a consequent increase of the reactive force. This effect is more evident in figure 35 where the installation of guide vanes, which caused a more uniform discharge velocity, decreased the thrust at a given volume rate of discharge. The decrease in thrust, however, was more than compensated by the reduction in pressure so that the net result of the guide vanes was beneficial, as previously stated.

A reduction of the geometric area of the opening relative to the area of the duct at the pressure tap would be expected, in general, to increase the static-pressure coefficients. Such a tendency is shown in figures 36 and 37. Departure of the static-pressure coefficients from zero for the openings in which $A/A_d = 1$, moreover, was due in part to the reduction of effective jet area as well as to the bend losses. This slight reduction of the effective jet area at the openings made the agreement between theory and experiment for both the drag and the pressure characteristics appear to be poorer in these cases than it would have been if all comparisons were based upon the jet velocity ratio K_o rather than upon Q/AV.

Wing openings.- The outlet characteristics of openings in the NACA 0018 wing are presented in figures 38 and 39. If the theoretical curve of C_{PL_o} against H/q (fig. 24) is compared with the curves of figure 38, it will be seen that the power-loss coefficient of opening WREA is slightly less than the theoretical at all values of p/q. At low values of p/q, the discrepancy may have been due to a decrease in the friction drag behind the openings; but, at high values of p/q, the discrepancy was primarily due to a static-pressure recovery between the resistance and the outlet which was not considered in the observations or in the method of reduction but which is present also in many conventional radiator installations. The magnitude of this pressure recovery was estimated from the curves of figure 6 and was found to be sufficient to account for the discrepancy.

The power-loss coefficient of the adjustable-flap openings at 0.800c was somewhat above that of the fixed openings over the complete range of flow or pressure. The external loss of the adjustable-flap openings was largely responsible for the difference, as may be seen from a comparison of drag curves. It will be noticed that, in the wing tests of the adjustable-flap openings both as inlets and outlets and at both 0.175c and 0.800c, the openings with the smallest gaps did not have the lowest power-loss coefficients. The relatively high power-loss coefficients of these openings were probably due to the use of 1/16-inch, square-edge plate for all models; the ratio of plate thickness to height of opening was 0.50 for the smallest gap.

The external drag of adjustable-flap openings at 0.175c was expected to be much higher than that of similar openings at 0.800c, as was found in tests of the inlet openings. The outlet openings located at 0.175c necessitated a 180° change in flow direction that was expected to give a higher internal loss than openings at 0.800c. These increases in both the external and the internal losses of the outlet openings at 0.175c relative to those at 0.800c would tend to make the power-loss coefficients of the 0.175c openings higher than those of the 0.800c openings. Yet a comparison of the results given in figures 38 and 39 shows that the observed power-loss coefficients at the forward location were lower up to pressure coefficients of about 0.4 and were even below the theoretical values at pressure coefficients below 0.1. These low power-loss co-

efficients occurring at low discharge velocities were thought to have been due to a reduction in the frictional drag on the wing behind the openings, the effect of which was credited to the openings. Further experiment is required to verify this theory.

DESIGN RECOMMENDATIONS

Velocity Decreasing Systems

Inlet openings.- The inlet opening of an internal-flow system that tends to decrease the final velocity of the air flowing through it should, if practicable, be located at the forward stagnation point of some portion of the aircraft. The results of the present investigation indicate that openings so located may incur negligible losses, but no satisfactory inlet openings for other locations were developed. The investigation showed that small openings may cause relatively large losses; it will probably be found desirable to employ a common inlet opening for two or more systems when possible.

It is recommended that, whenever practicable, the inlet opening of a velocity-decreasing system be located in the highest total-pressure region of the propeller slipstream. Such a treatment promises more effective cooling on the ground and in climb and a small increase in efficiency at cruising and top speed.

Ducts.- Unnecessary duct losses should be carefully avoided. Such losses will generally entail additional wake losses. Many references pertaining to duct design are available, the gist of which may be condensed into the following general principle: Avoid high velocities and abrupt changes of the shape or the area of cross section except at the outlet. Butterfly valves or other throttling devices within the ducts or at the inlet should be avoided. Regulation at the outlet is practicable and efficient. Leakage should be eliminated because it will generally cause large increases in airplane drag. It appears desirable to test all internal-flow systems, including the airplane cabin, for leakage.

Outlet openings.- For the minimum power-loss coefficient of an outlet opening, the hypothetical jet velocity

should be the same as that of the potential flow at the location of the opening (that is, $K_o = 1$). When the outlet velocity is considerably below the optimum, which may be the result of large pressure losses within the system, it may be advantageous to install a blower.

On pusher-propeller installations it appears desirable to locate the outlet openings of velocity-decreasing systems ahead of the propeller in order to increase the propulsive efficiency. This recommendation is not limited to internal-flow systems, but its desirability in connection with bodies such as wings or fuselages is already well known. Additional research on pusher-propeller arrangements appears desirable.

Velocity-Increasing Systems

Many internal-flow systems tend to increase the final velocity of the air flowing through them. Such systems assist in propelling the aircraft and may therefore be considered as a part of the propulsive system. Similar to propellers, systems of this type may be most efficient when located in the wake of velocity-decreasing systems, including wings and fuselages; a narrow-slot inlet opening in a region of relatively thick boundary layer appears promising and should be further investigated. When the required quantity of air is large relative to the quantity that can be obtained from the boundary layer, however, an inlet located at a forward stagnation point will probably be found to be the most efficient.

The outlet velocity of a propulsive system will seldom be appreciably less than that of the free stream. In general, therefore, the outlet shape and location should be such that the jet will not impinge on the external surfaces of the aircraft.

Langley Memorial Aeronautical Laboratory,
National Advisory Committee for Aeronautics,
Langley Field, Va., August 1, 1940.

REFERENCES

1. Meredith, F. W.: Note on the Cooling of Aircraft Engines with Special Reference to Ethylene Glycol Radiators Enclosed in Ducts. R. & M. No. 1683, British A.R.C., 1936.

2. Weick, Fred E.: Aircraft Propeller Design. McGraw-Hill Book Co., Inc., 1930, ch. 2.

3. Capon, R. S.: The Cowling of Cooling Systems. R. & M. No. 1702, British A.R.C., 1936.

4. Wenzinger, Carl J., and Harris, Thomas A.: The Vertical Wind Tunnel of the National Advisory Committee for Aeronautics. Rep. No. 387, NACA, 1931.

5. Wirt, Loring: New Data for the Design of Elbows in Duct Systems. Gen. Elec. Rev., vol. 30, no. 6, June 1927, pp. 286-296.

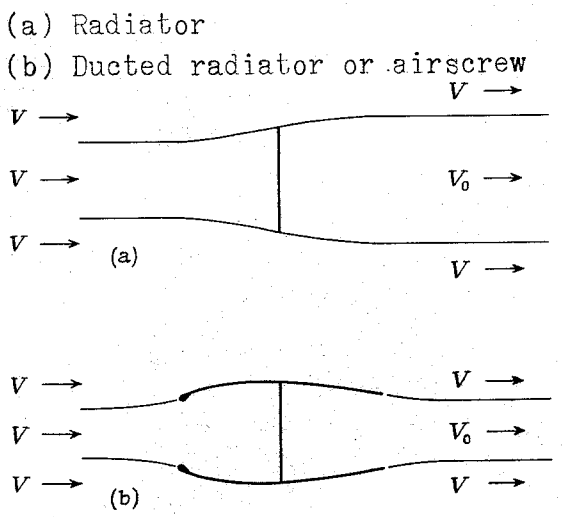

Figure 1.- Isolated internal-flow systems.

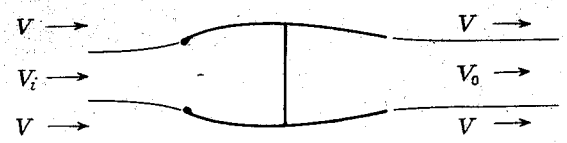

Figure 2.- Internal-flow system in slipstream or wake.

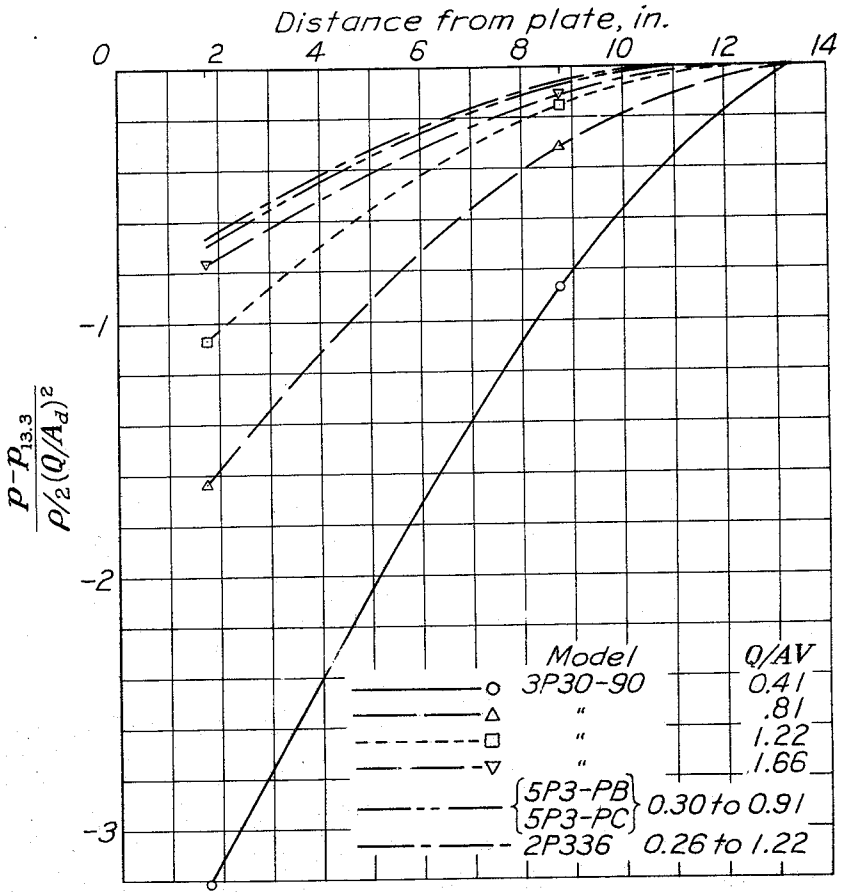

Figure 8.- Inlet duct pressure gradients. See figures 13,15,and 16 for model dimensions. ($p_{13.3}$ is static pressure 13.3 inches from plate).

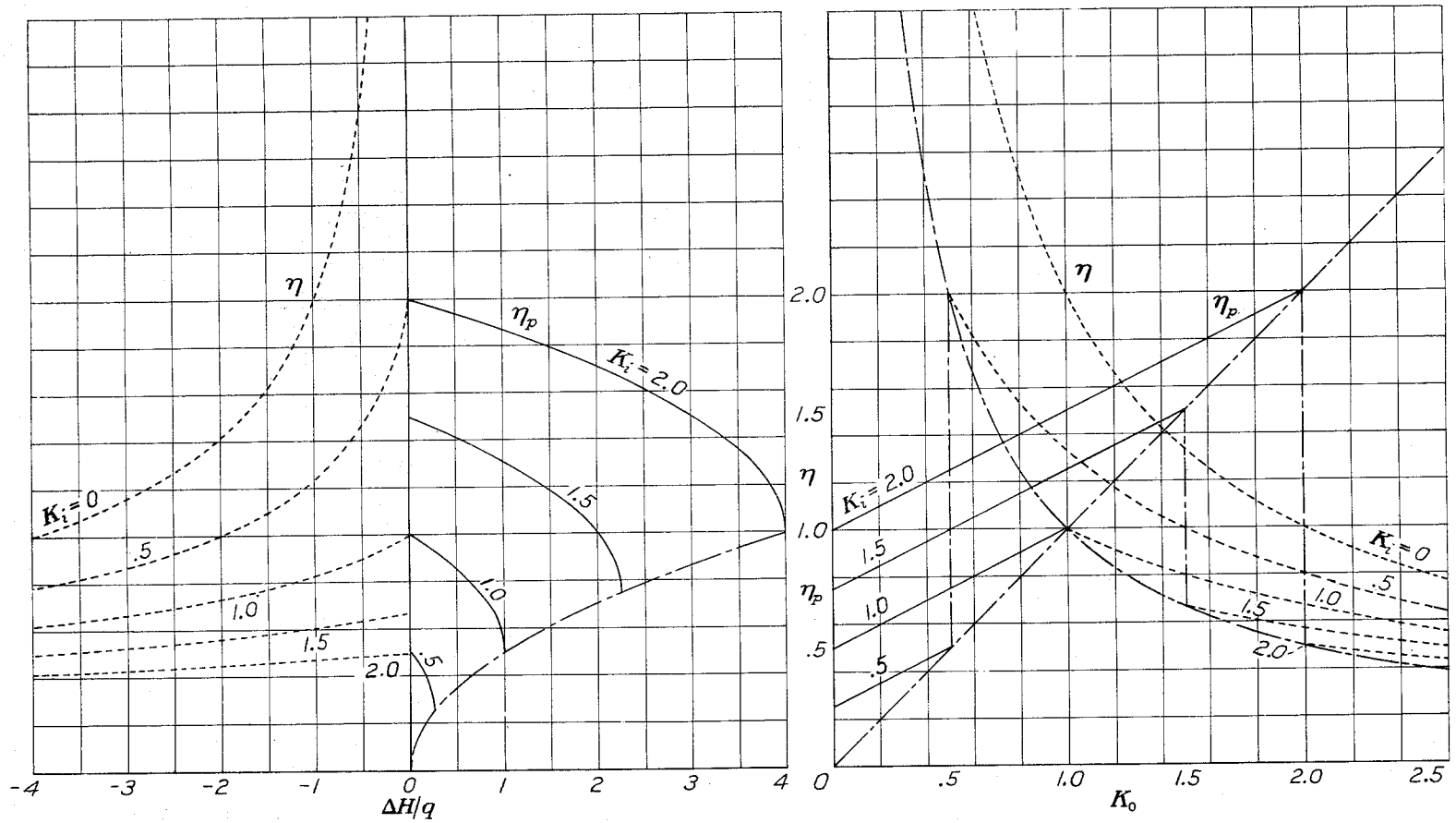

$$\eta_p = \frac{K_i + K_o}{2} = \frac{K_i + \sqrt{K_i^2 - \frac{\Delta H}{q}}}{2}$$ represented by continuous curve

$$\eta = \frac{2}{K_i + K_o} = \frac{2}{K_i + \sqrt{K_i^2 - \frac{\Delta H}{q}}}$$ represented by dotted curve

Figure 3.- Efficiency of an internal-flow system.

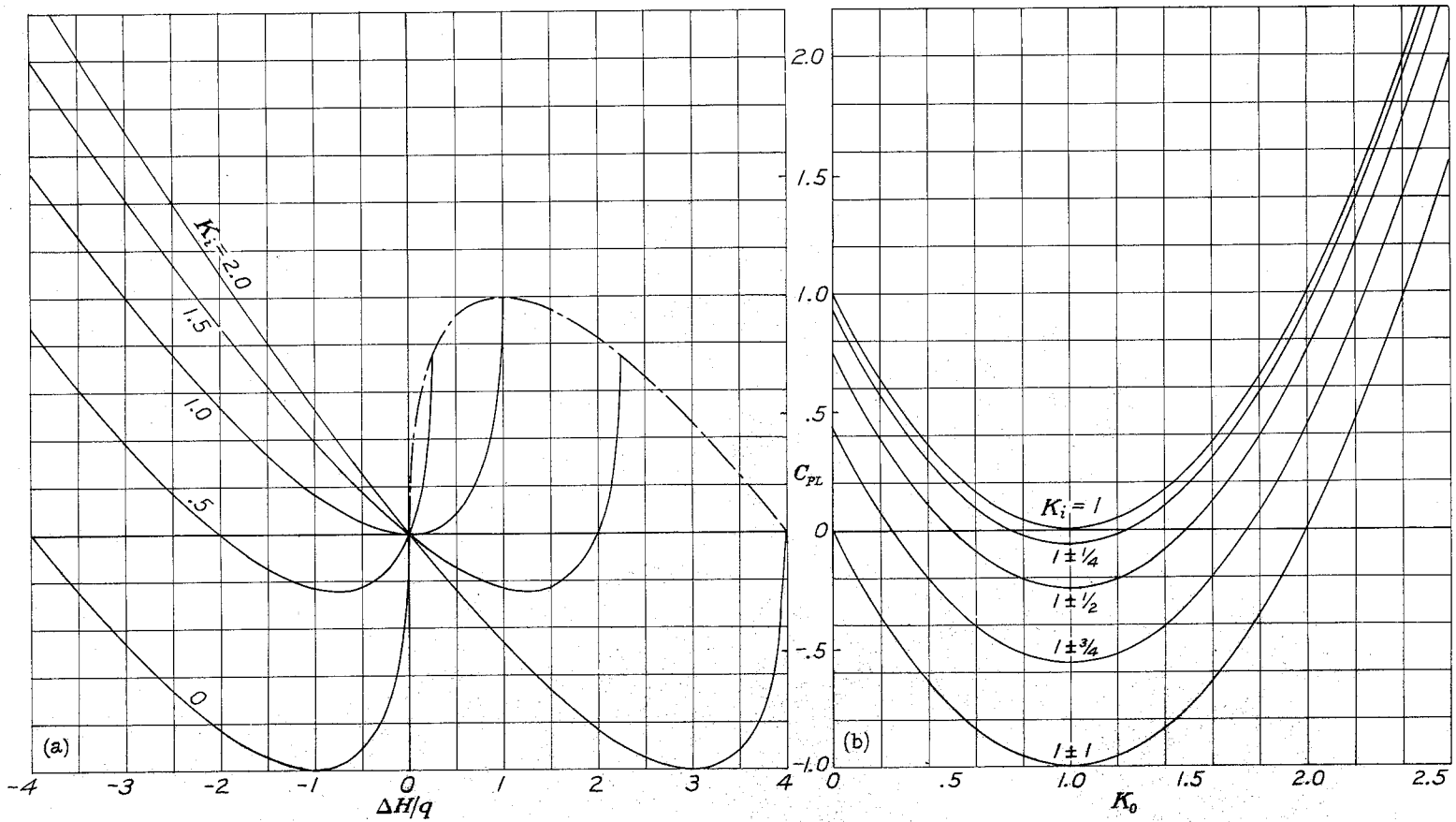

(a) $C_{PL} = 2\left(K_i - \sqrt{K_i^2 - \Delta H/q}\right) - \Delta H/q$ (b) $C_{PL} = (K_o - 1)^2 - (K_i - 1)^2$

Figure 4.- Power-loss coefficient of an internal-flow system.

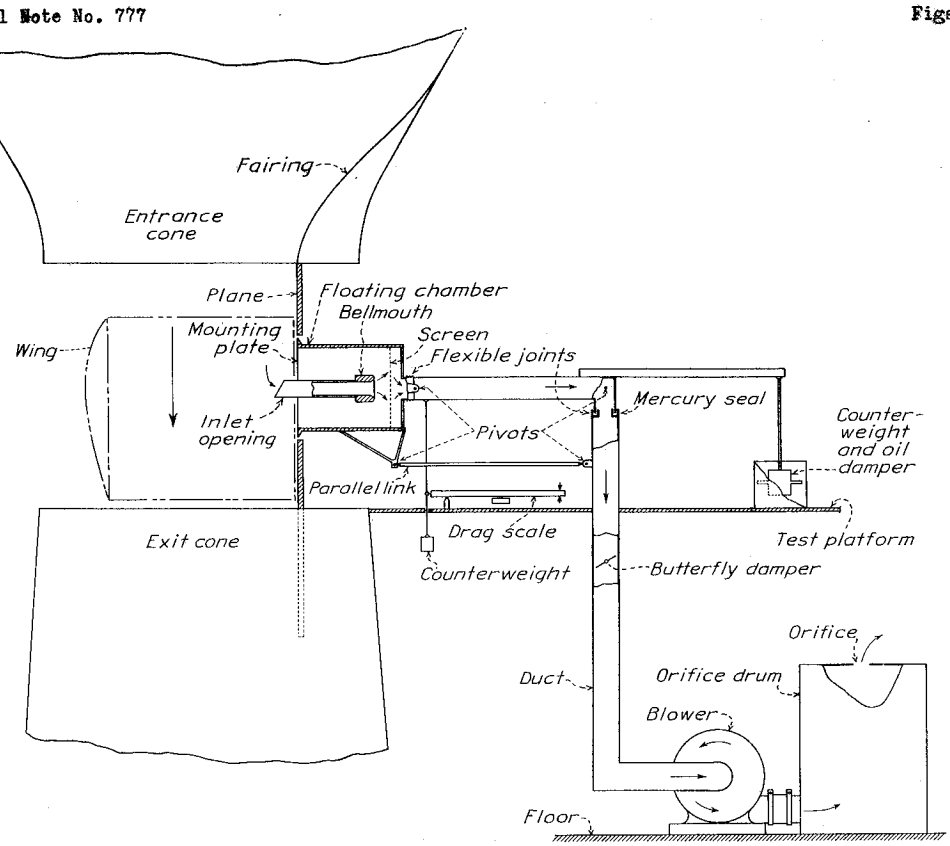

Figure 5.- The wind-tunnel set-up.

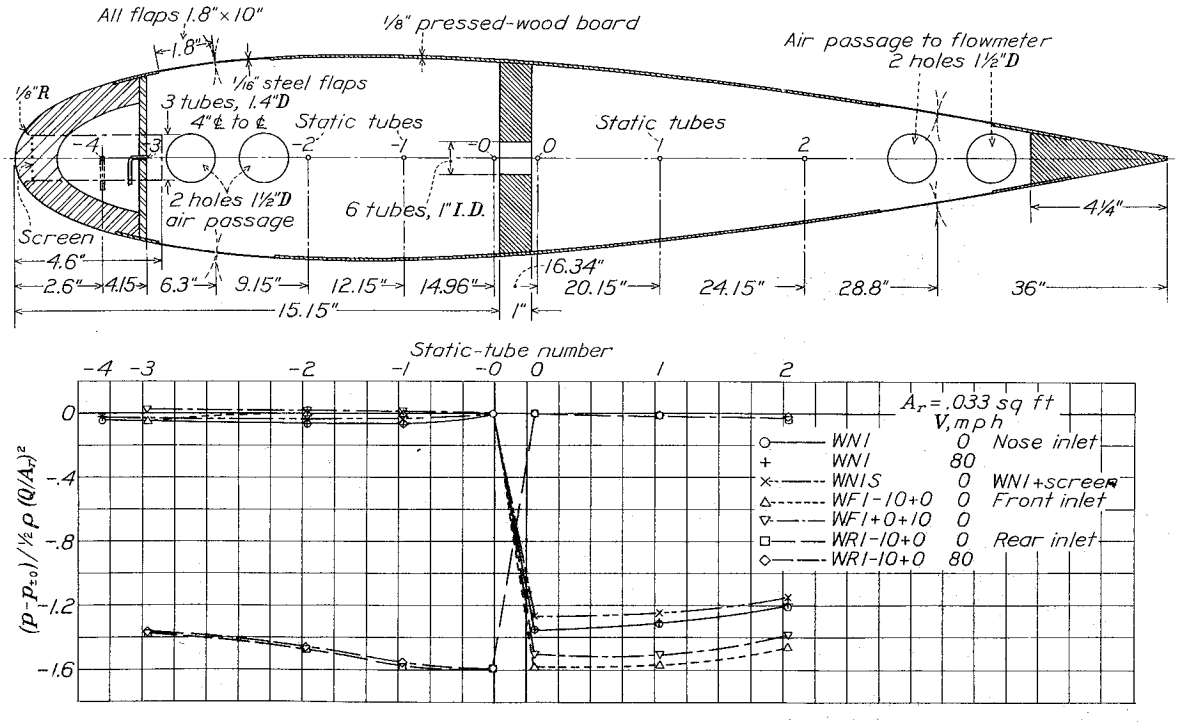

Figure 6.- Dimensions and pressure gradients of the central wing compartment.

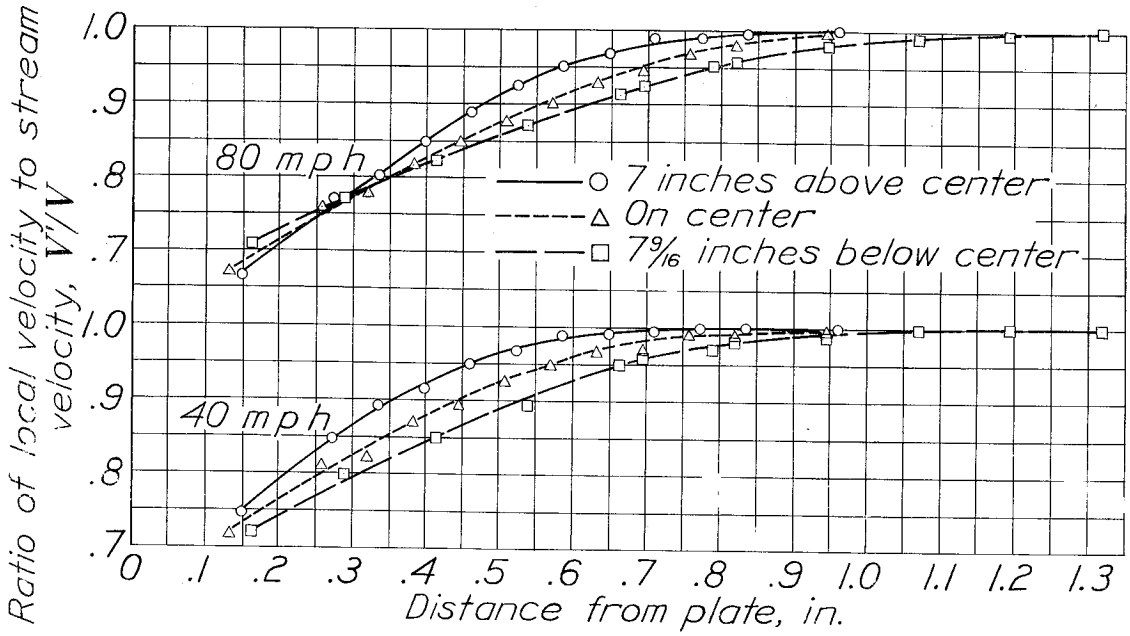

(a) On vertical center line of mounting plate without wing or openings.

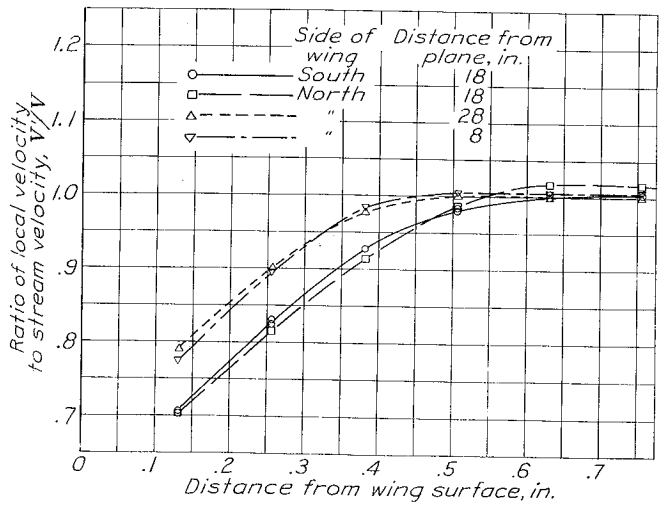

(b) At 0.800c on the wing with adjustable openings closed and sealed. V, 80 mph.

Figure 7.- Boundary layer velocity distributions.

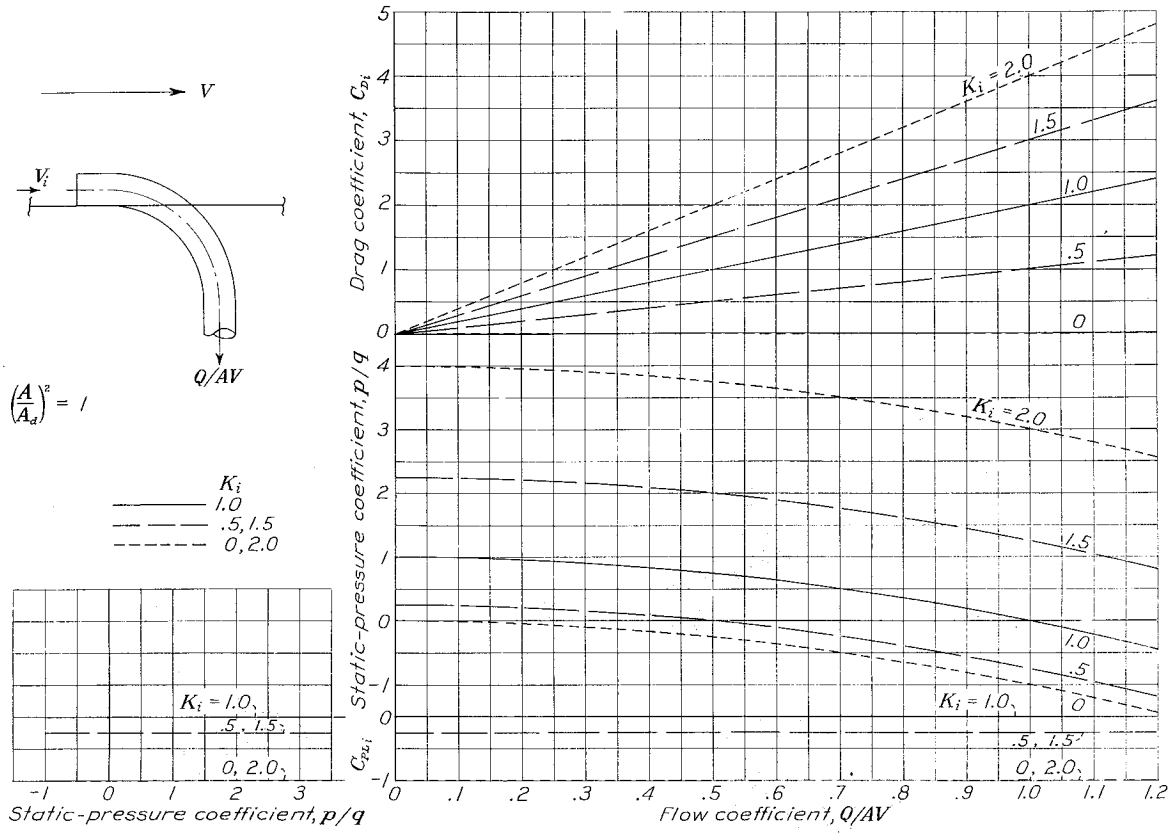

Figure 9.- Theoretical aerodynamic characteristics of an inlet opening in a flat plate.

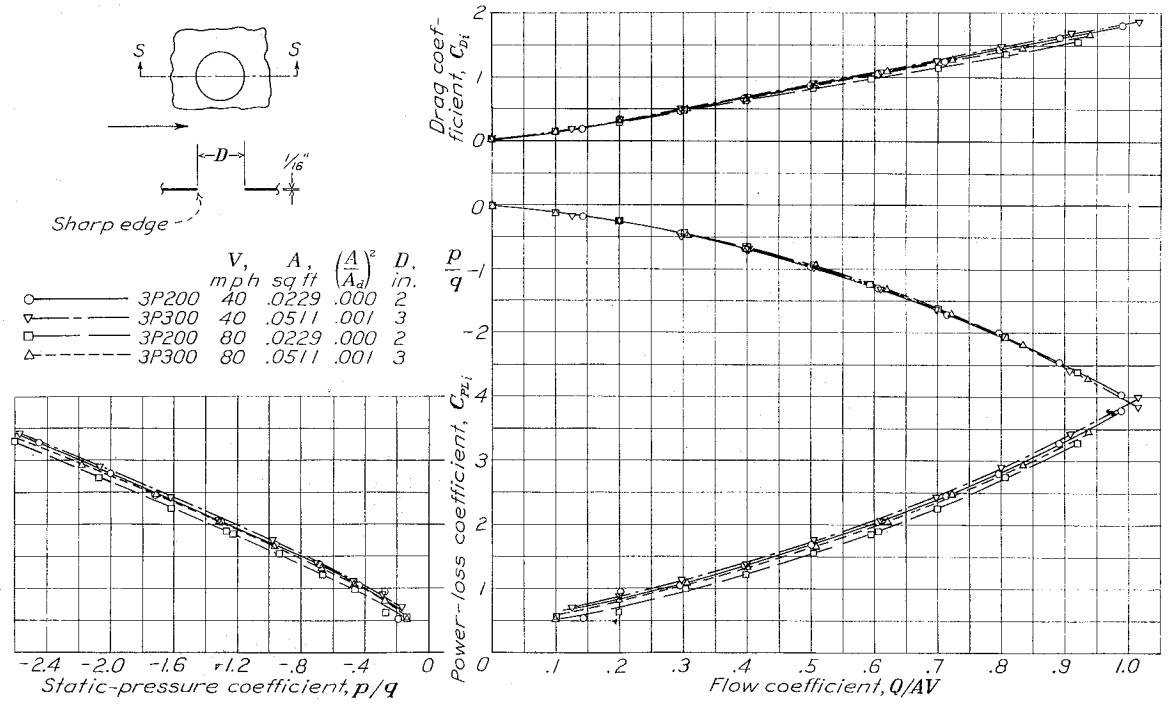

Figure 10.- Inlet characteristics of a circular hole in a flat plate.

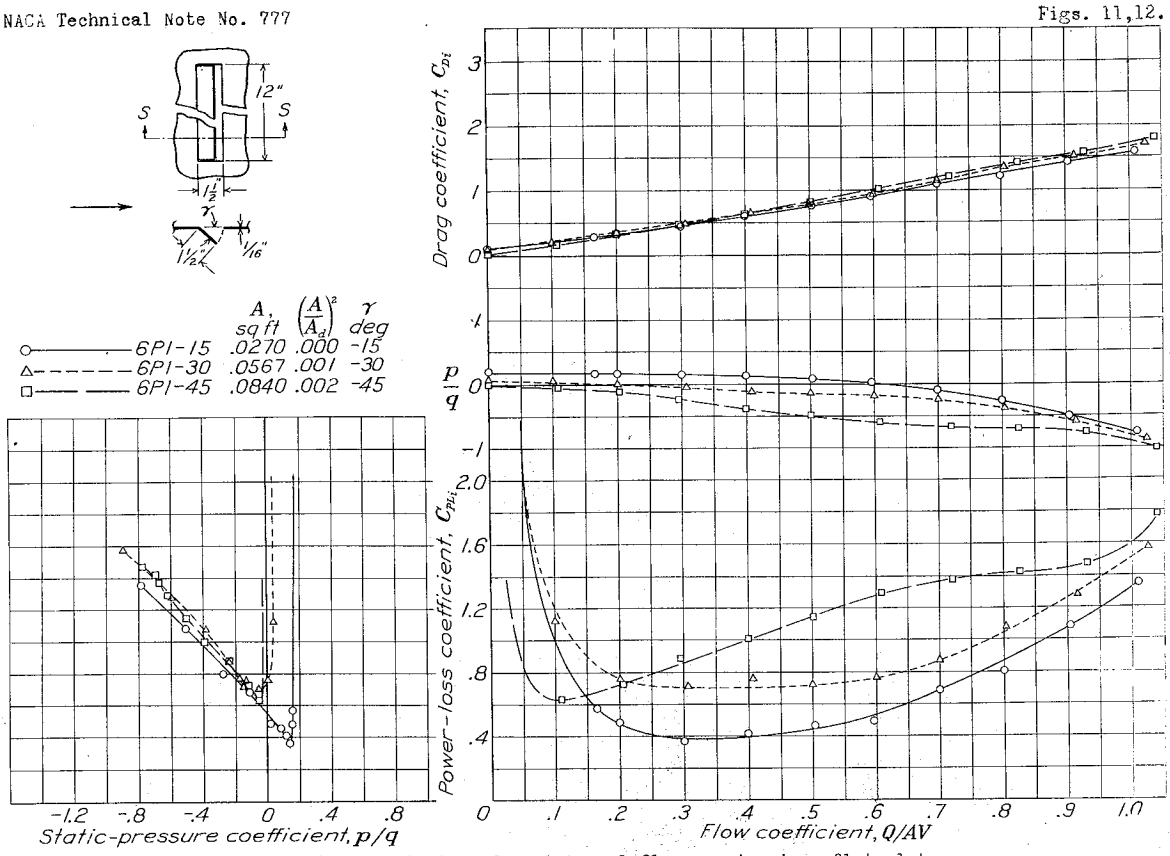

Figure 11.- Inlet characteristics of an internal-flap opening in a flat plate.

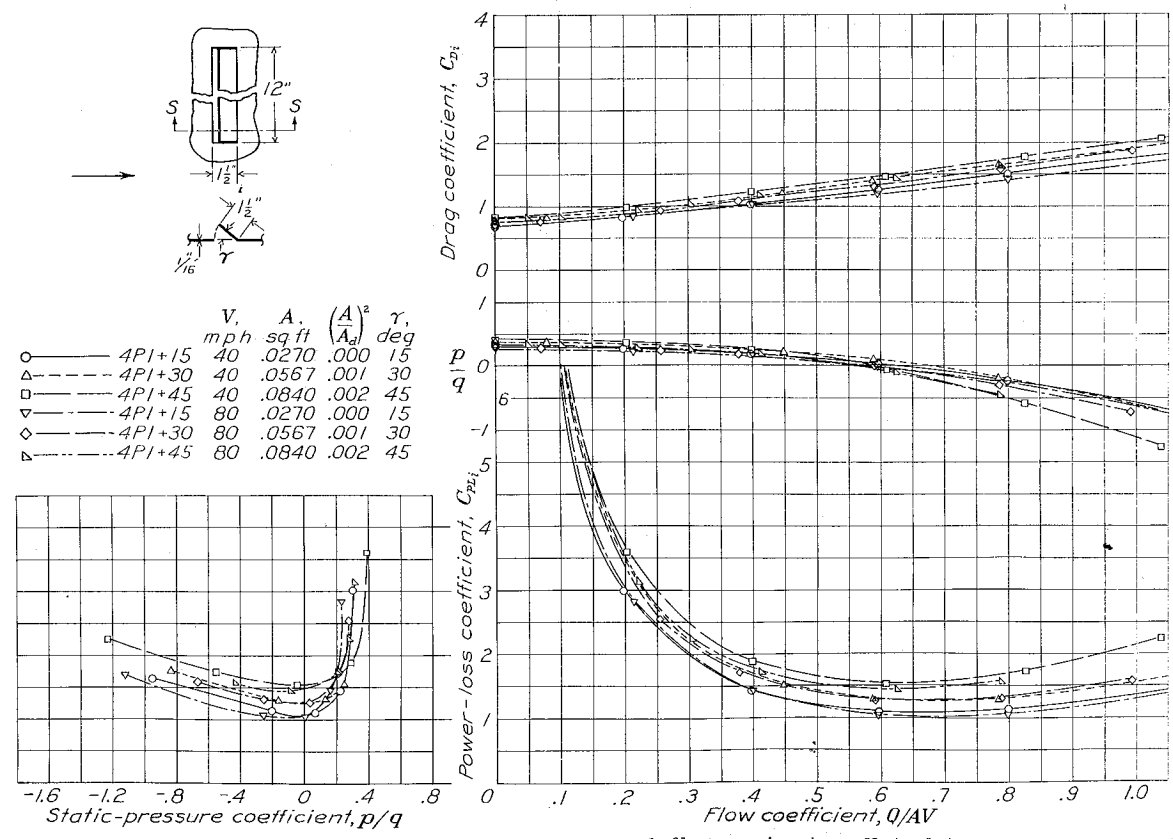

Figure 12.- Inlet characteristics of an external-flap opening in a flat plate.

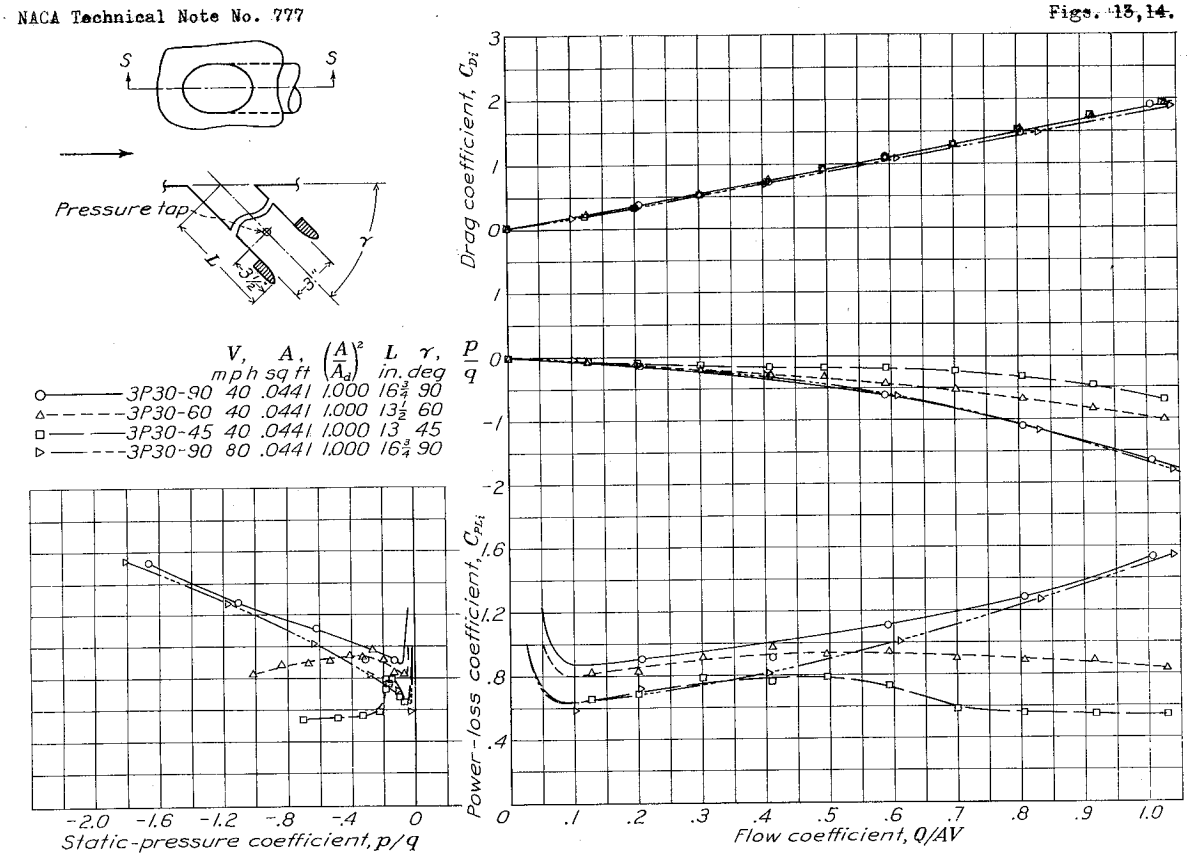

Figure 13.- Inlet characteristics of a flush circular duct in a flat plate.

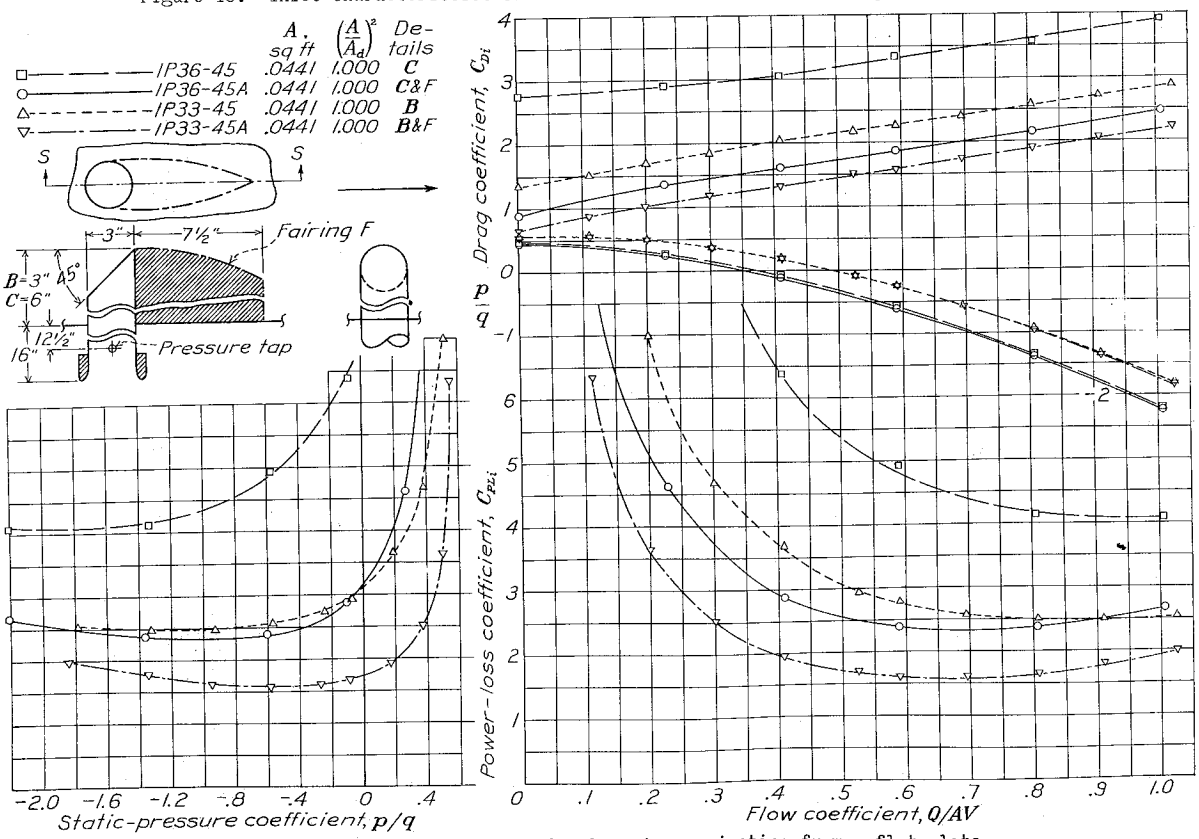

Figure 14.- Inlet characteristics of a circular pipe projecting from a flat plate.

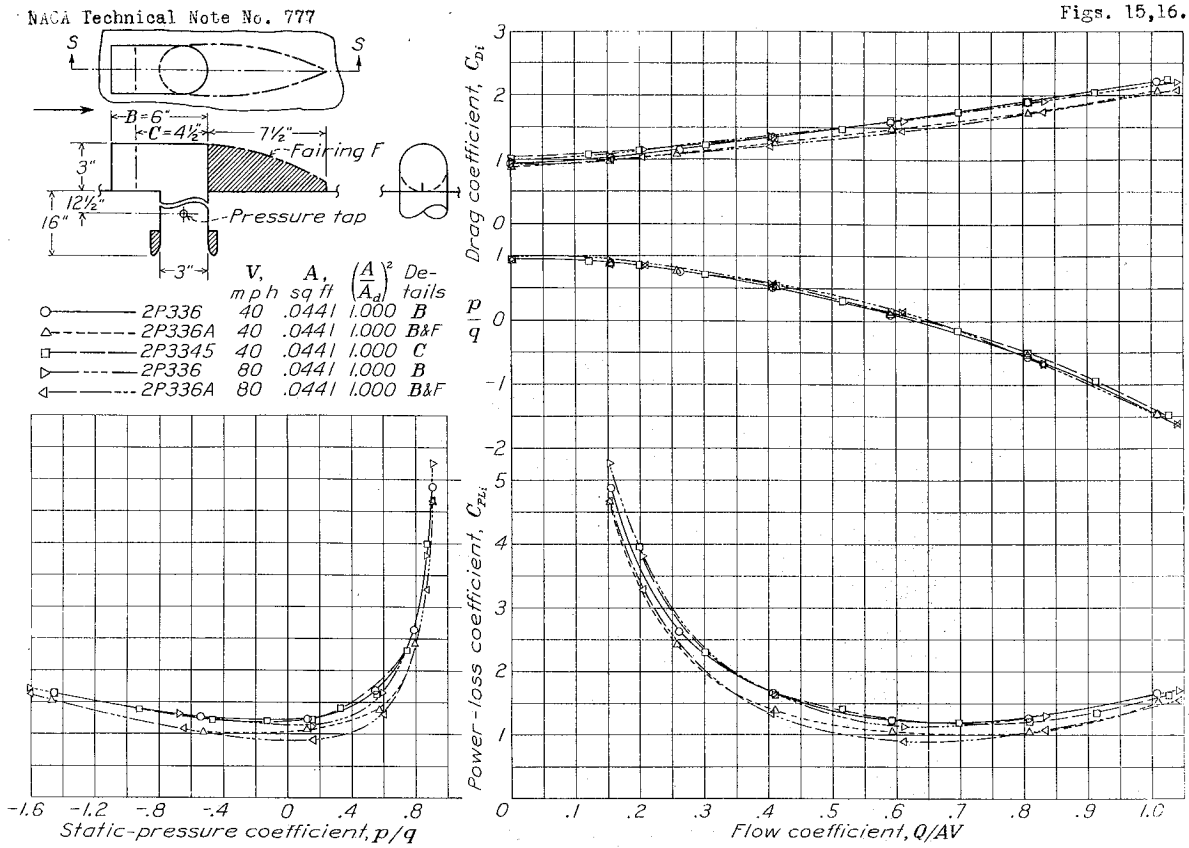

Figure 15.- Inlet characteristics of a circular pipe with an elbow projecting from a flat plate.

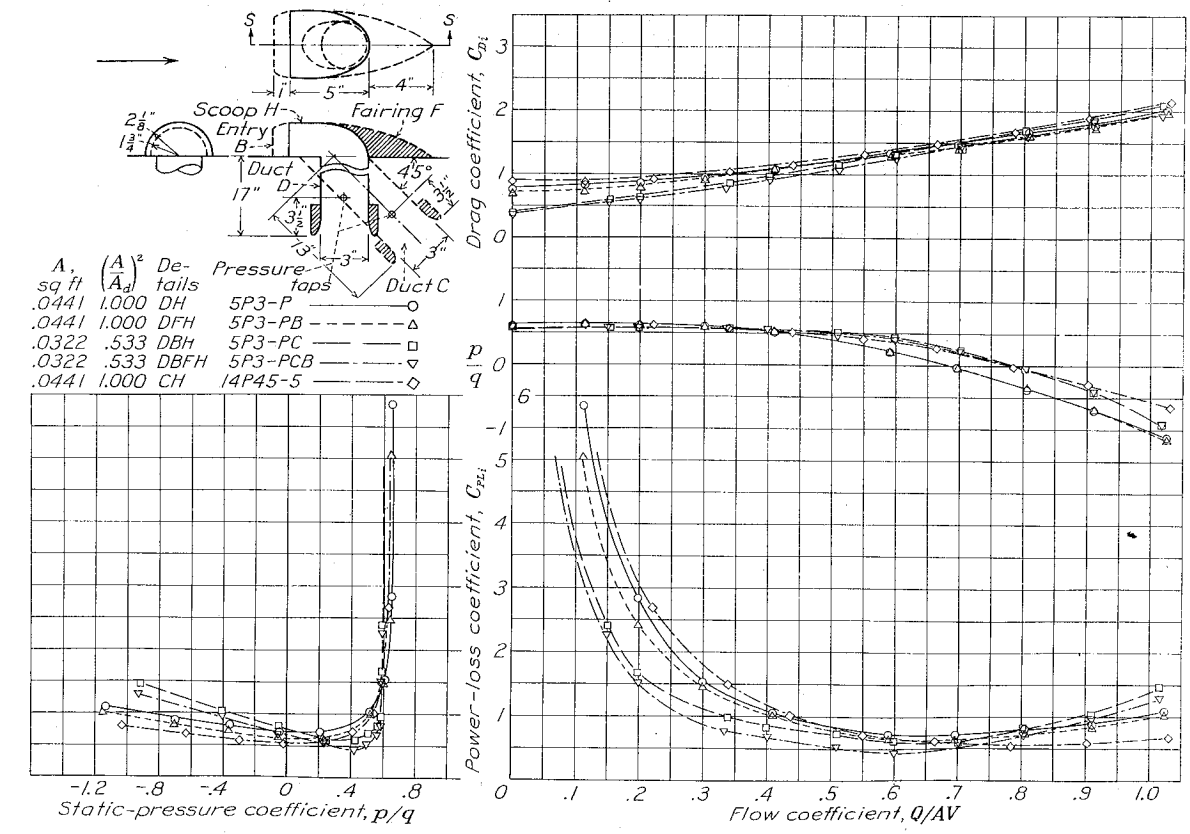

Figure 16.- Inlet characteristics of a scoop over a circular duct in a flat plate.

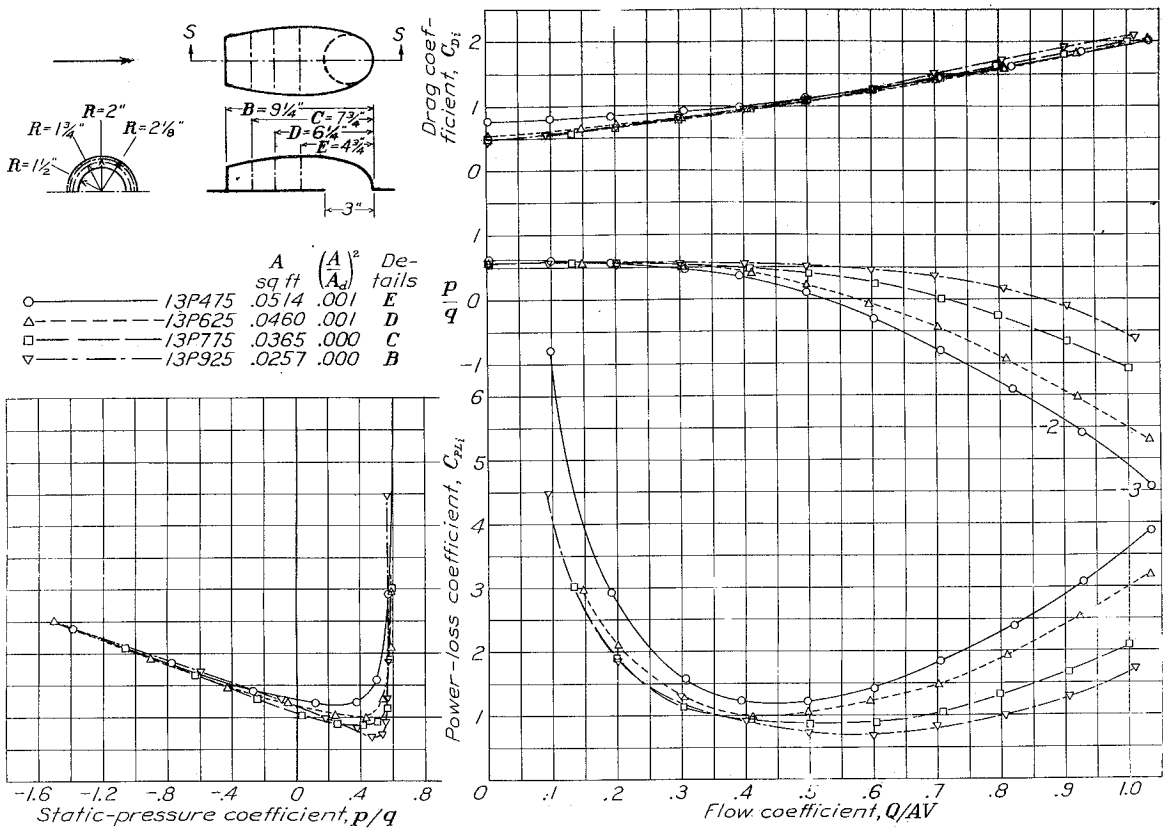

Figure 17.- Inlet characteristics of a scoop over a circular hole in a flat plate.

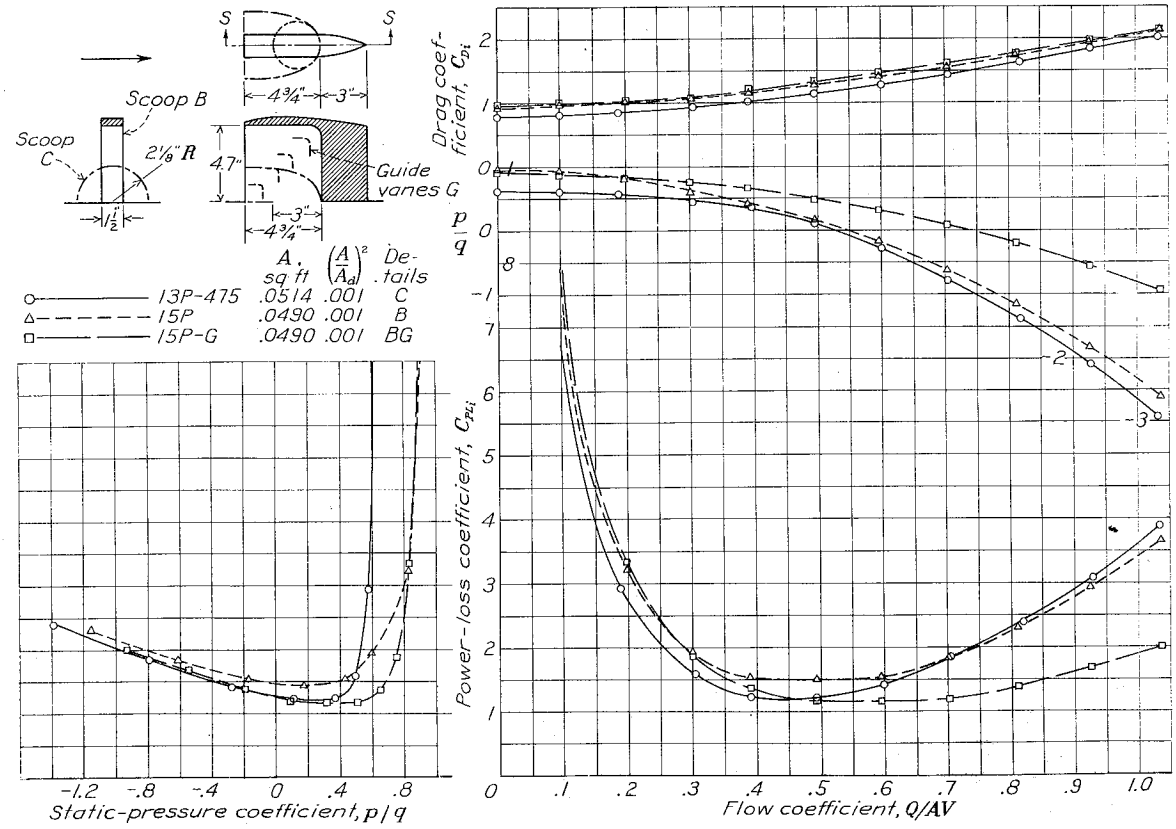

Figure 18.- Inlet characteristics of a high, thin scoop over a hole in a flat plate.

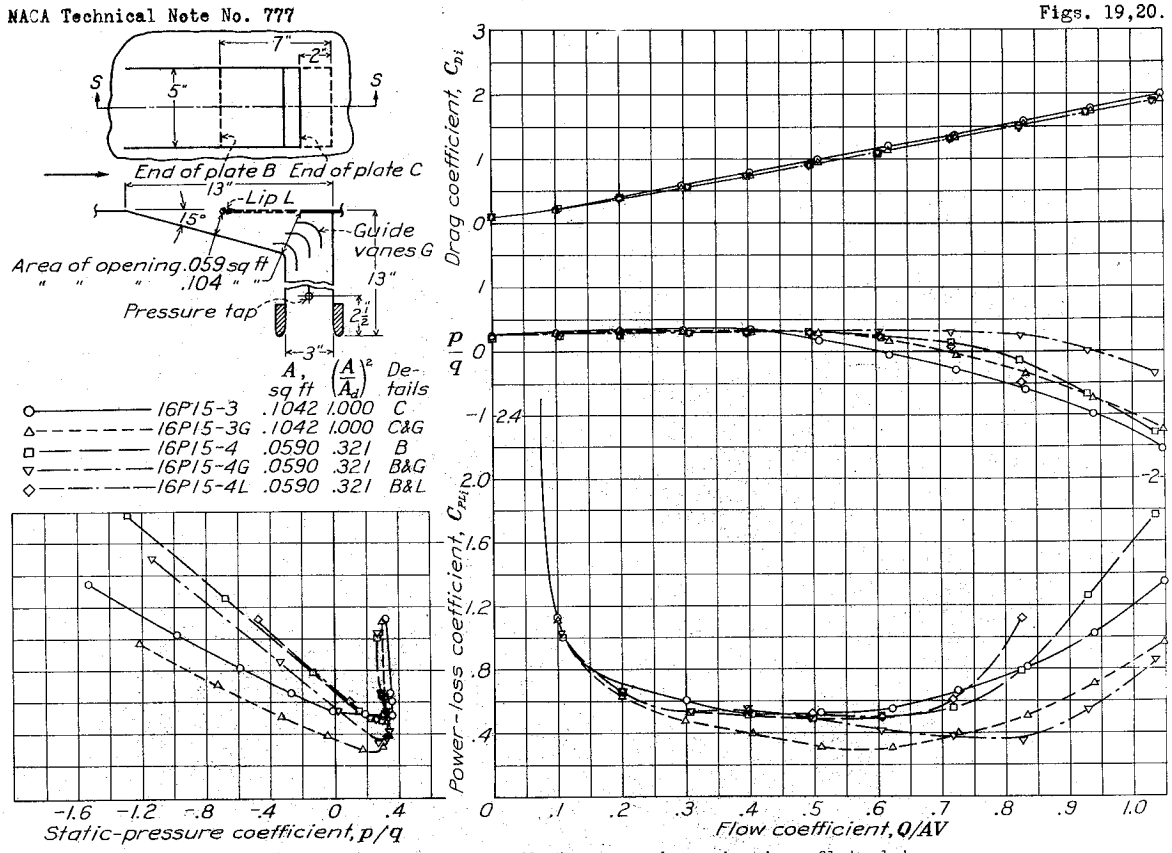

Figure 19.- Inlet characteristics of a flush recessed opening in a flat plate.

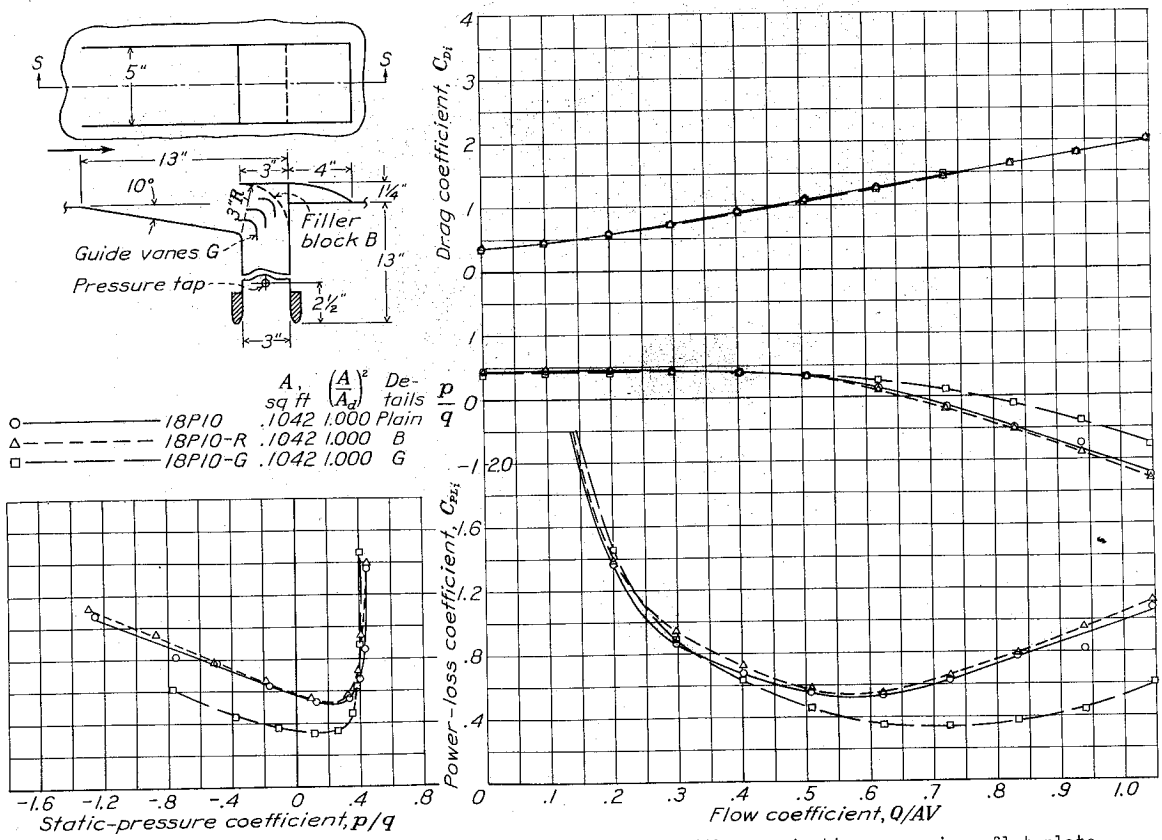

Figure 20.- Inlet characteristics of a recessed opening with a projecting scoop in a flat plate.

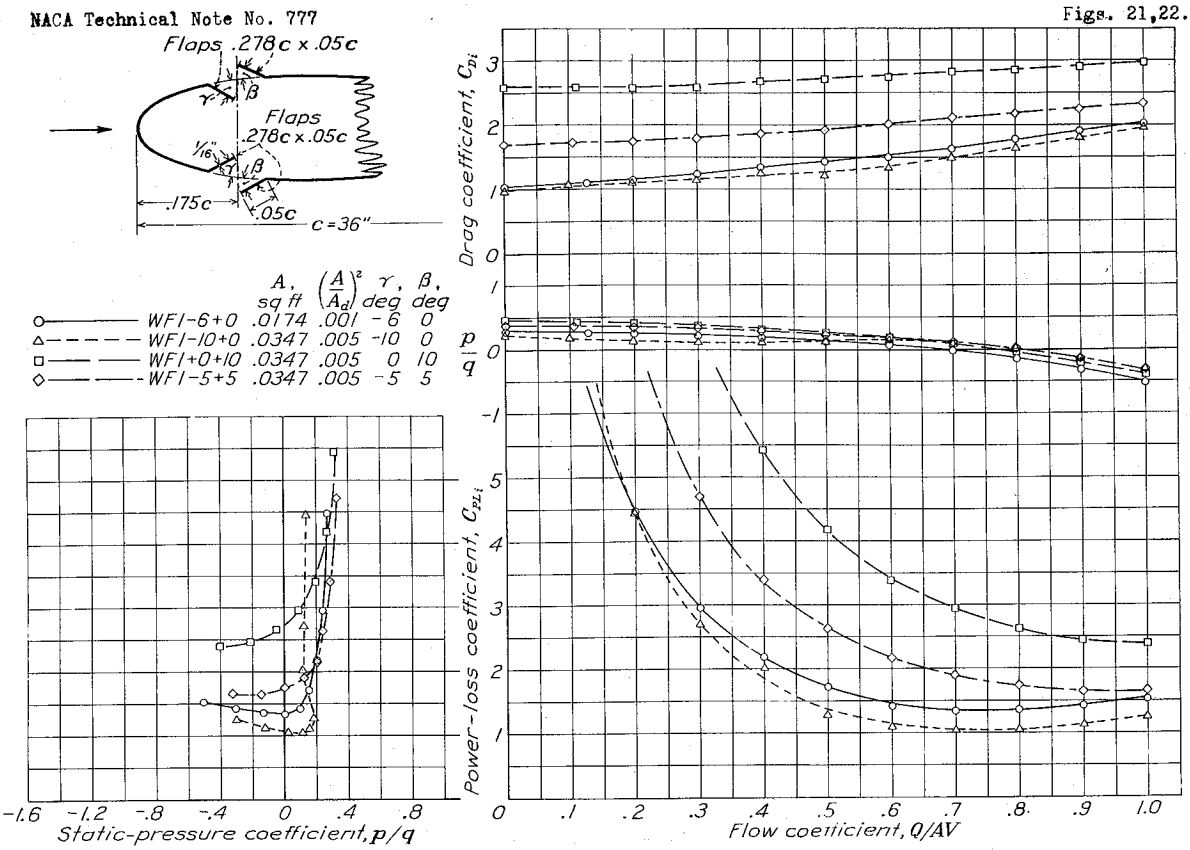

Figure 21.- Inlet characteristics of an adjustable-flap opening at 0.175c in an NACA 0018 wing.

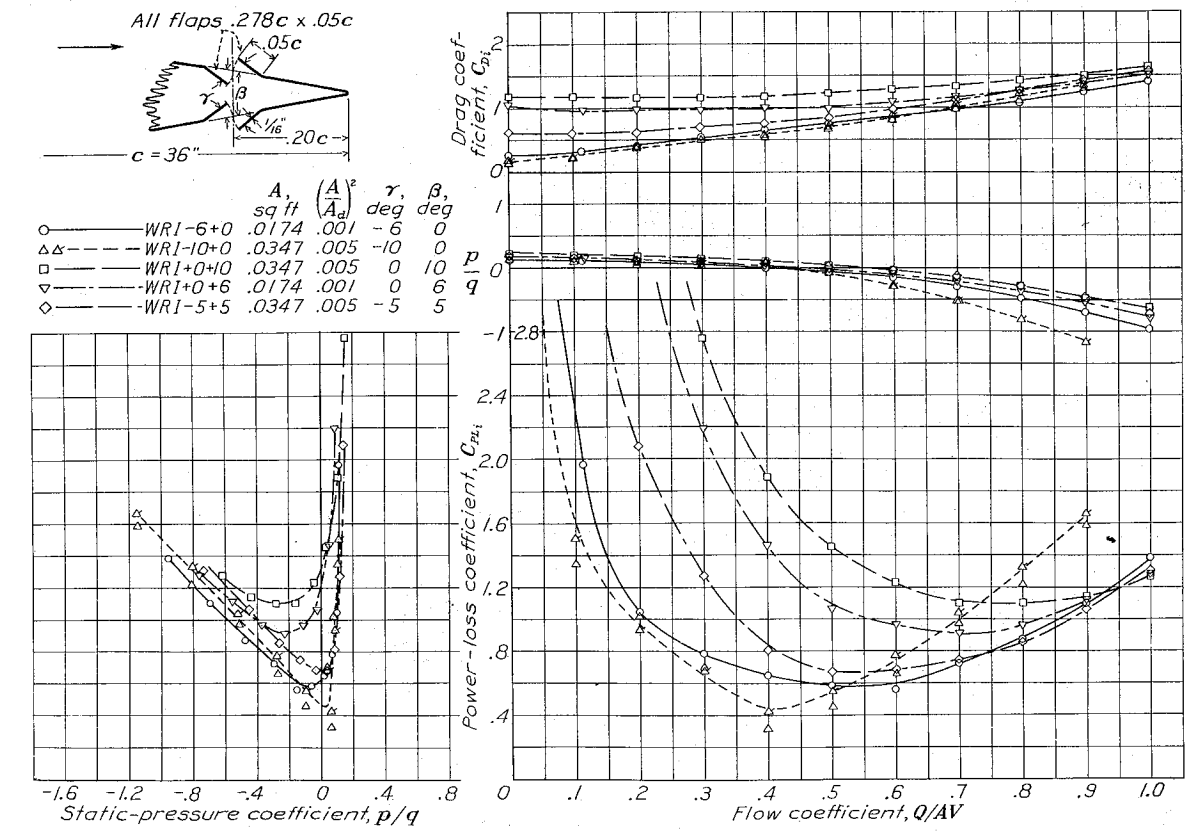

Figure 22.- Inlet characteristics of an adjustable-flap opening at 0.800c in an NACA 0018 wing.

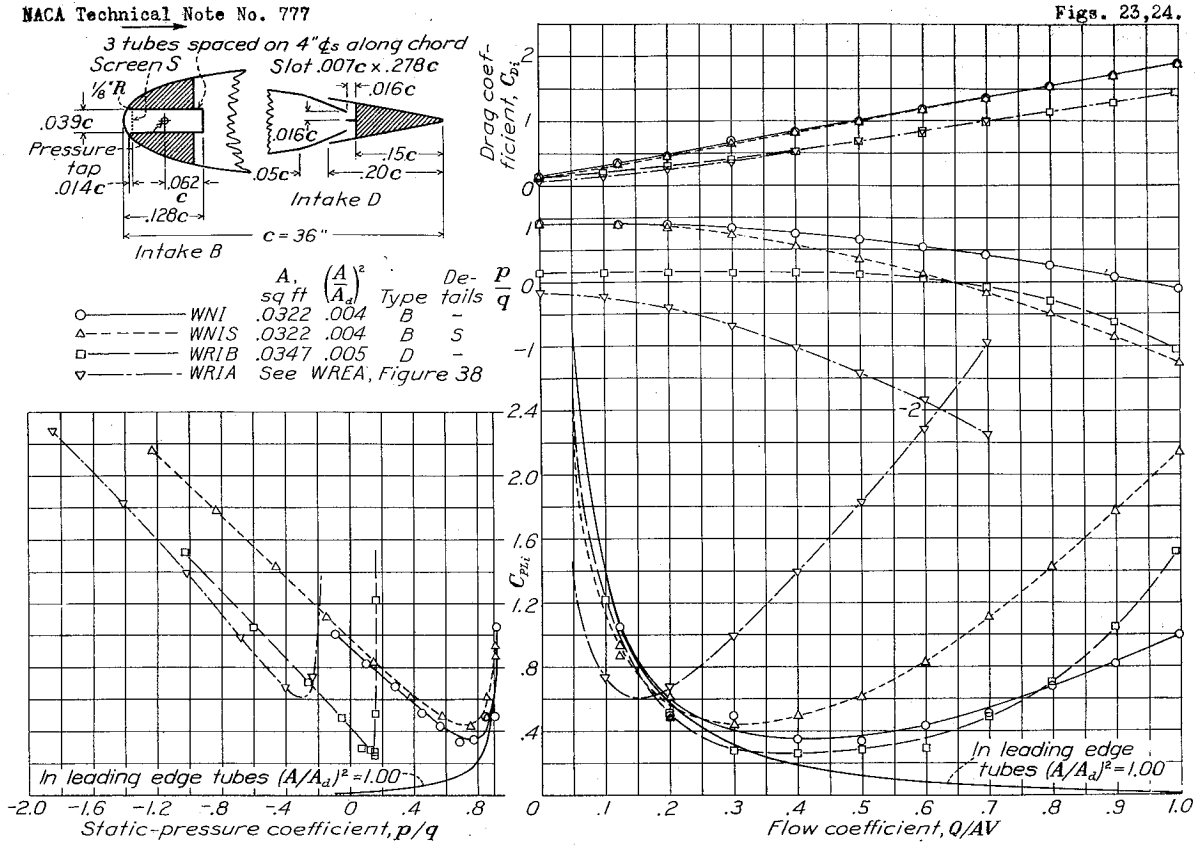

Figure 23.- Inlet characteristics of faired openings at the nose and at 0.800c in an NACA 0018 wing.

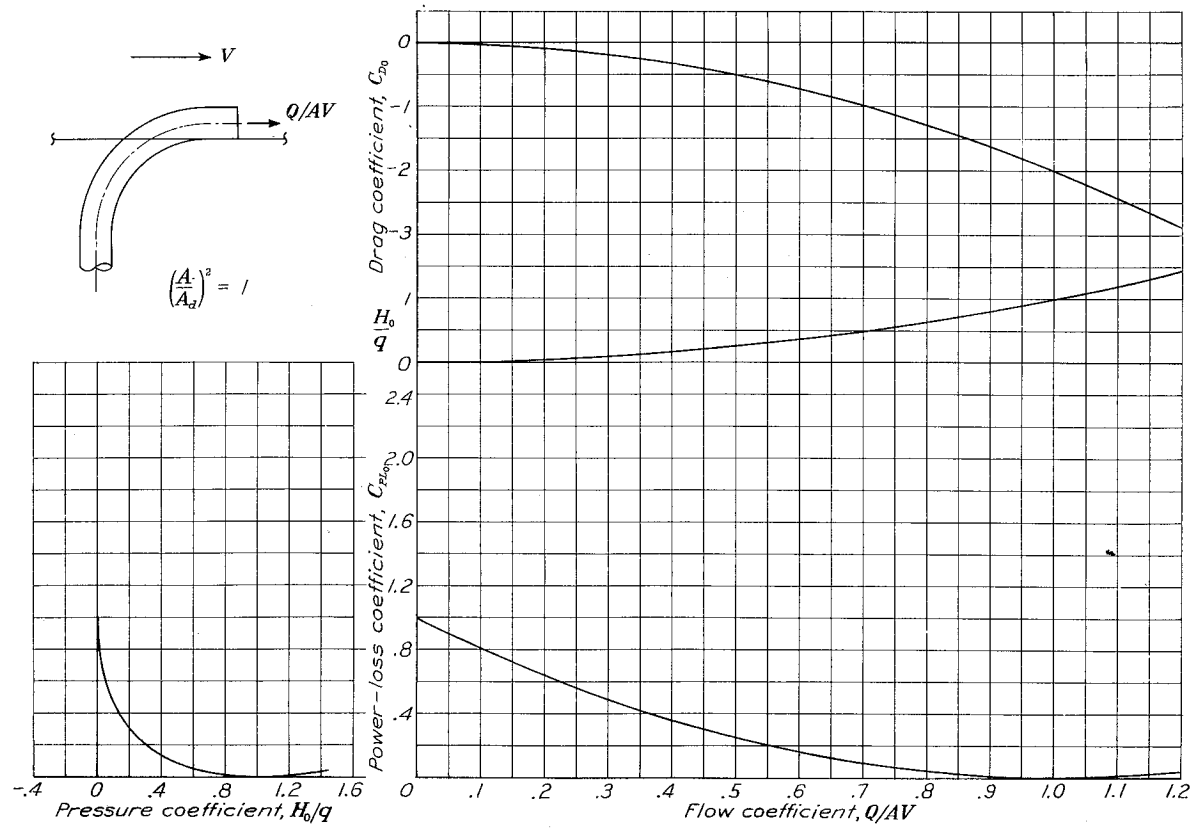

Figure 24.- Theoretical aerodynamic characteristics of an outlet opening in a flat plate.

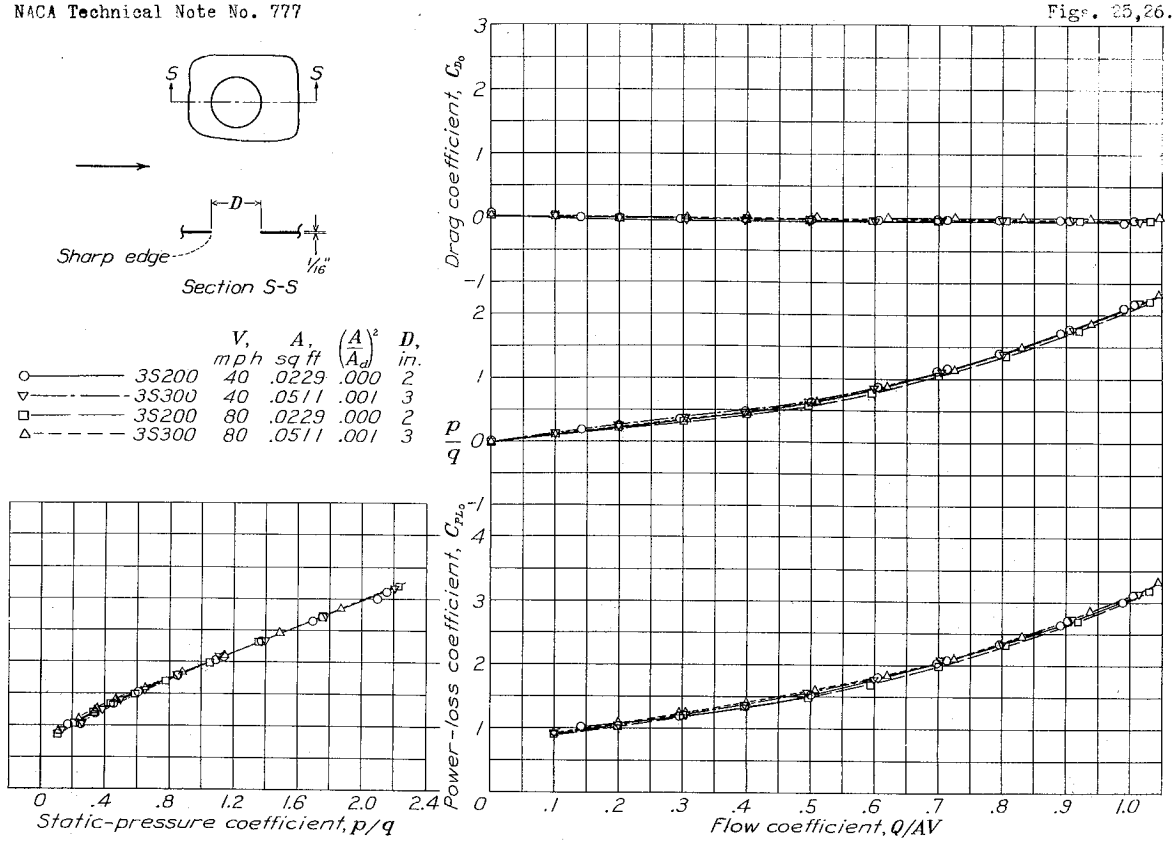

Figure 25.- Outlet characteristics of a circular hole in a flat plate.

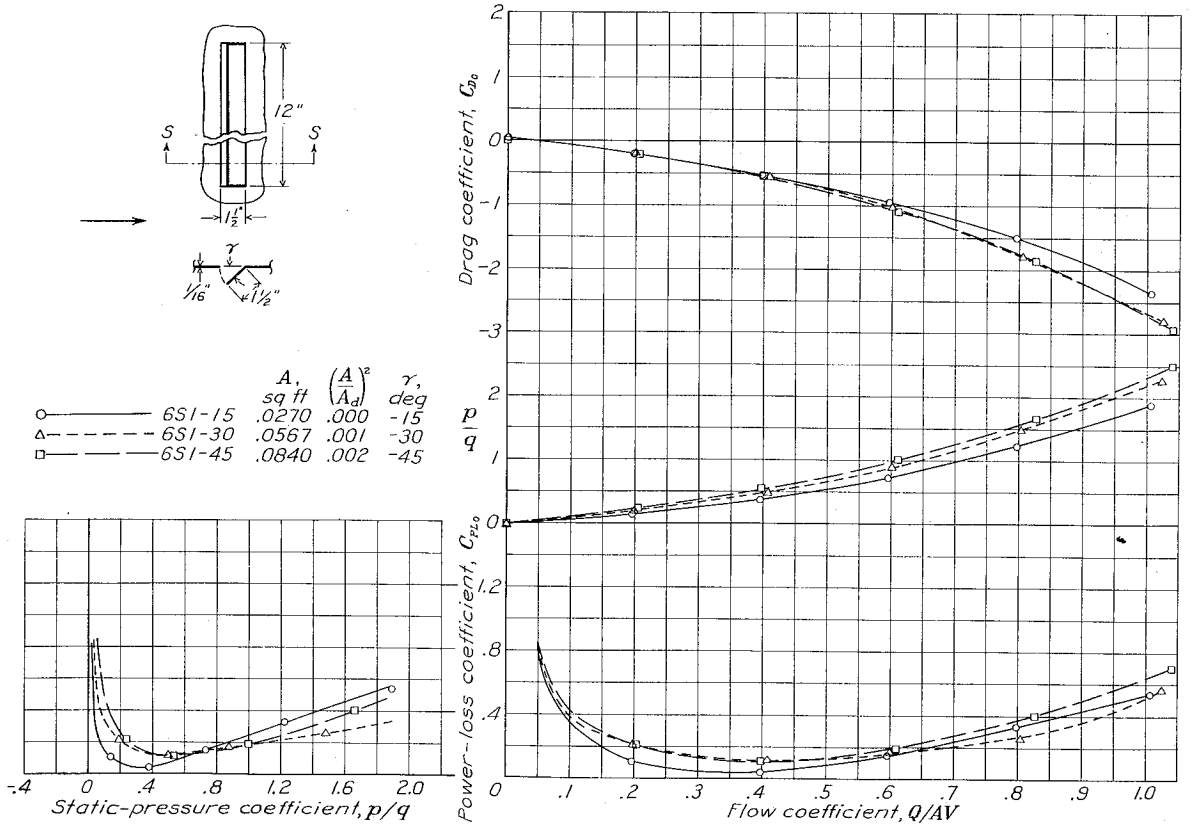

Figure 26.- Outlet characteristics of an internal-flap opening in a flat plate.

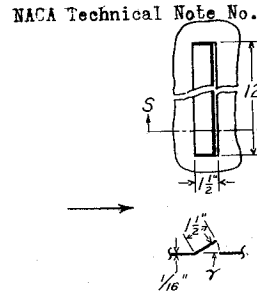

		V, mph	A, sq ft	$\left(\frac{A}{A_d}\right)^2$	γ, deg
○	45I+15	40	.0270	.000	15
△	45I+30	40	.0567	.001	30
□	45I+45	40	.0840	.002	45
▽	45I+30	80	.0567	.001	30

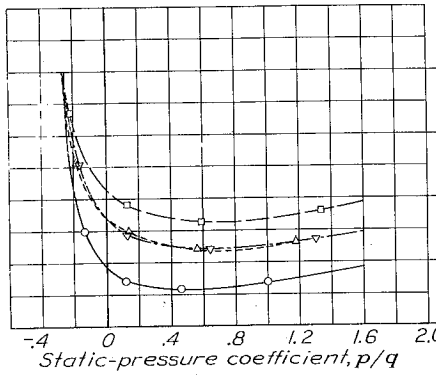

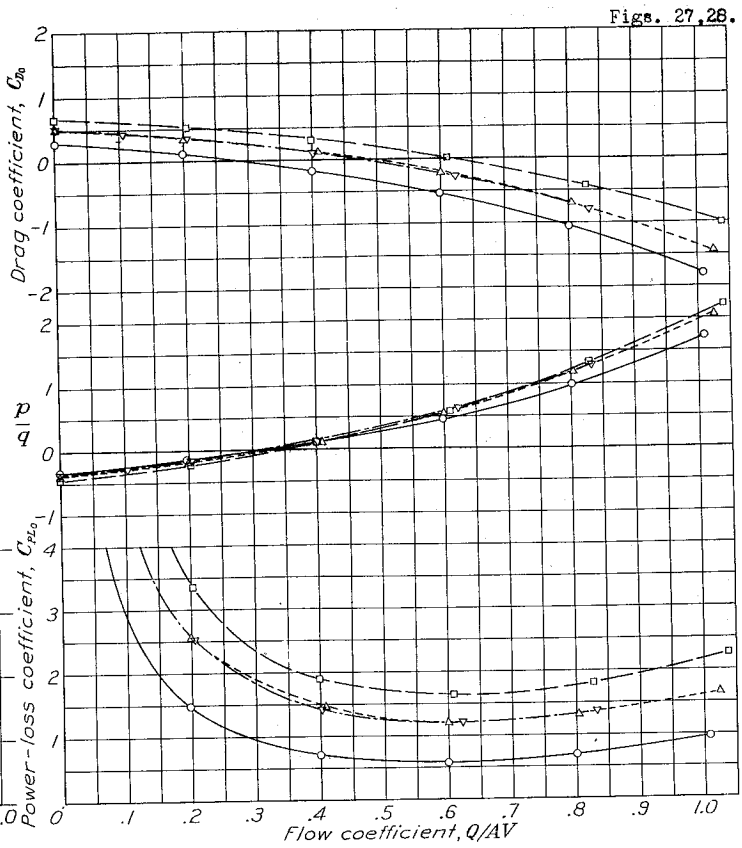

Figure 27.- Outlet characteristics of an external-flap opening in a flat plate.

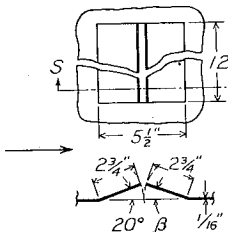

		A, sq ft	$\left(\frac{A}{A_d}\right)^2$	β, deg
△	7S+20+ 0	.0726	.002	0
○	7S+20+10	.0368	.000	10
□	7S+20+20	.0266	.000	20

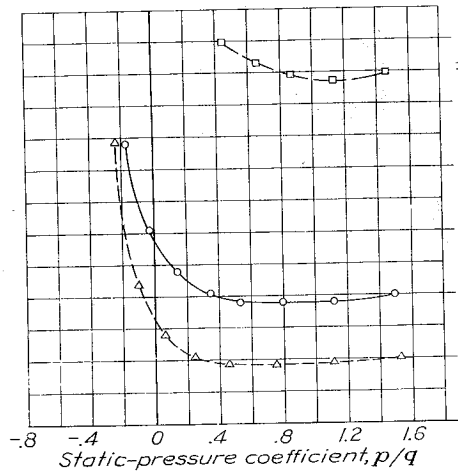

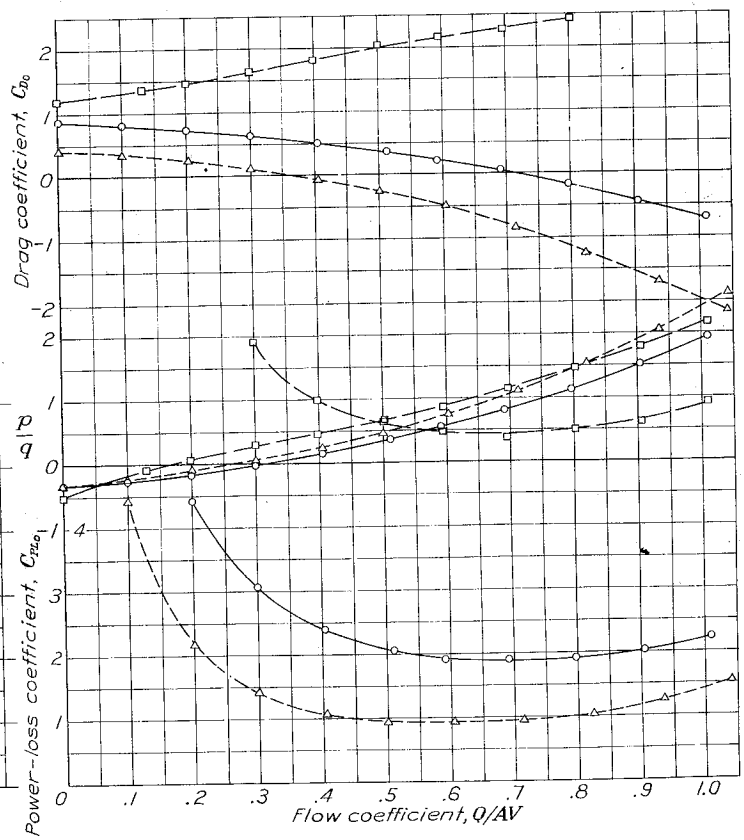

Figure 28.- Outlet characteristics of an opposed-flap opening in a flat plate.

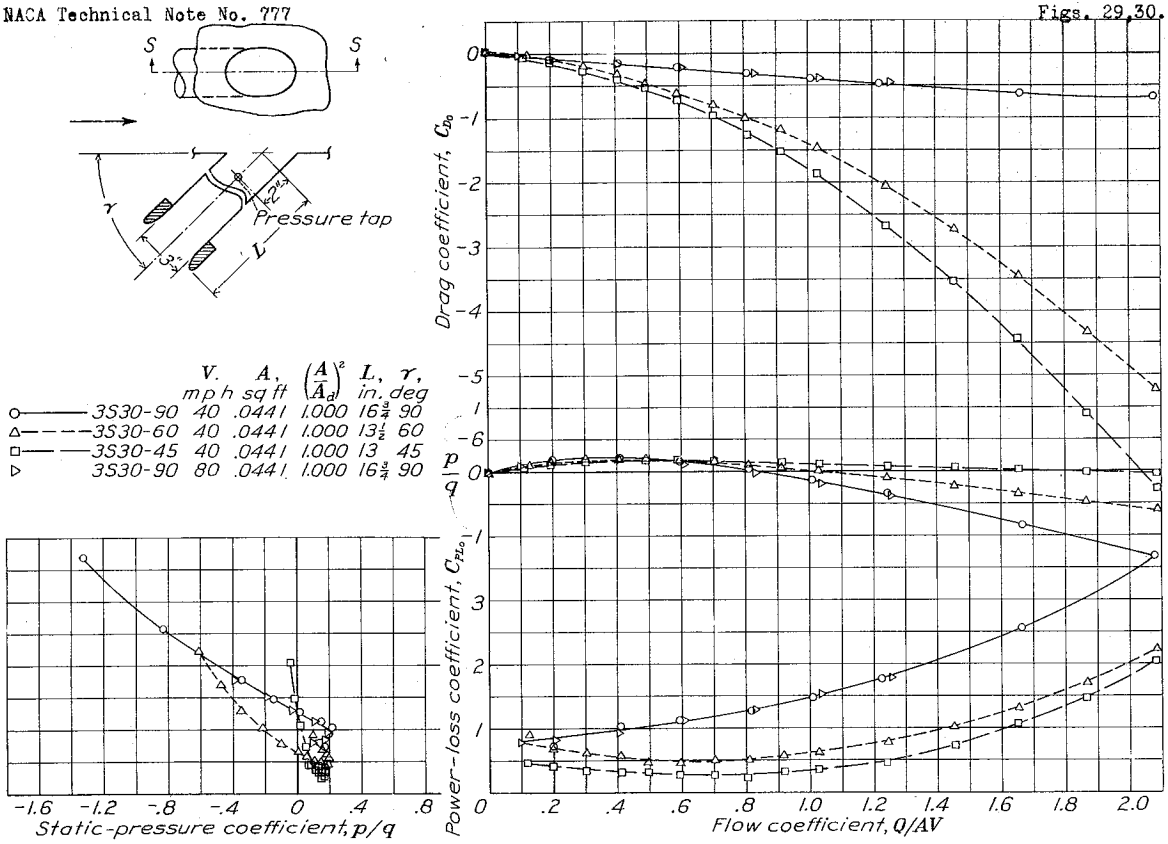

Figure 29.- Outlet characteristics of a flush circular duct in a flat plate.

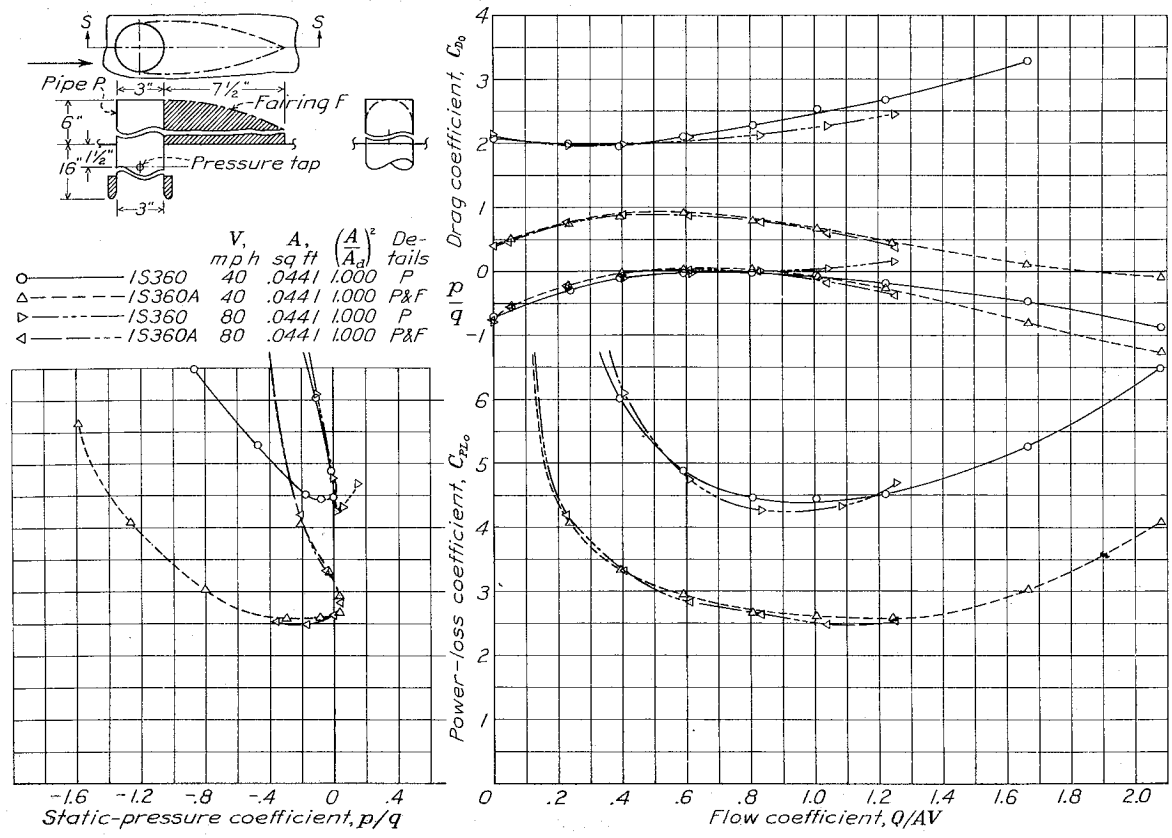

Figure 30.- Outlet characteristics of a circular pipe projecting from a flat plate.

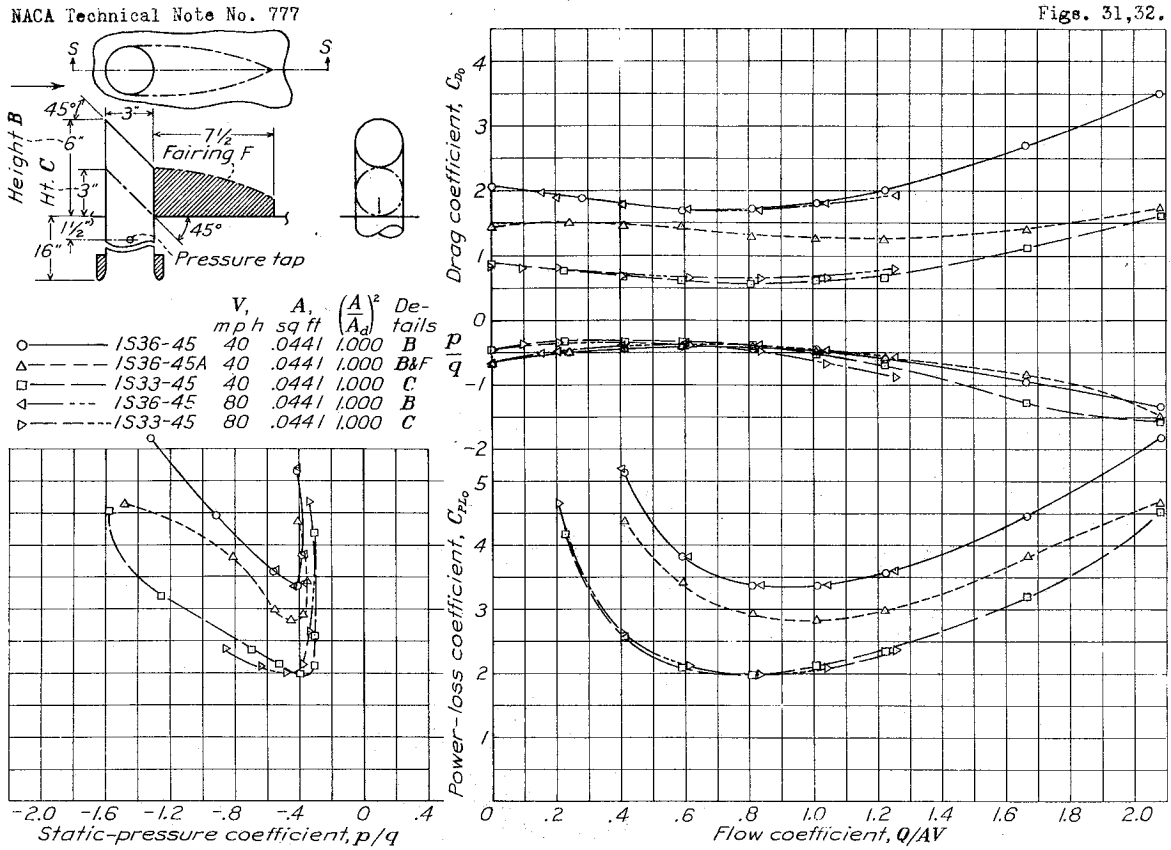

Figure 31.- Outlet characteristics of a circular pipe with 45° rake projecting from a flat plate.

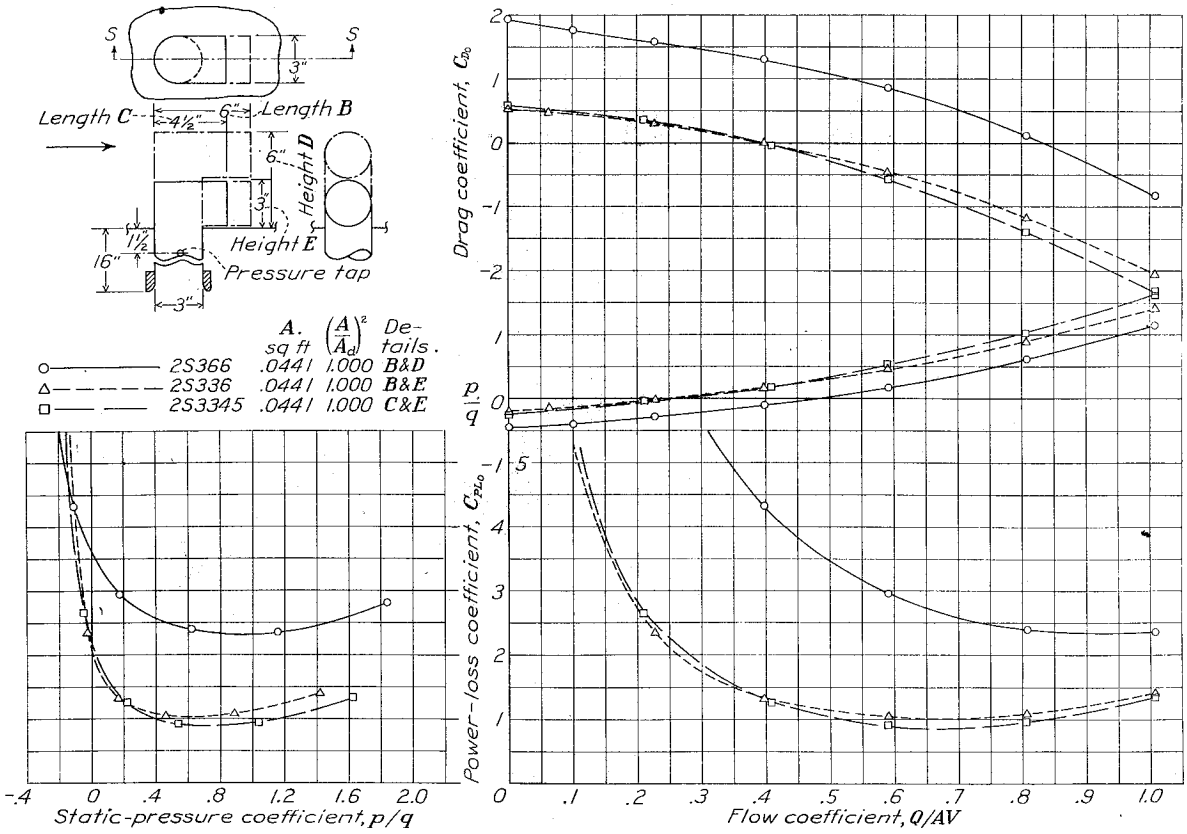

Figure 32.- Outlet characteristics of a circular pipe with an elbow projecting from a flat plate.

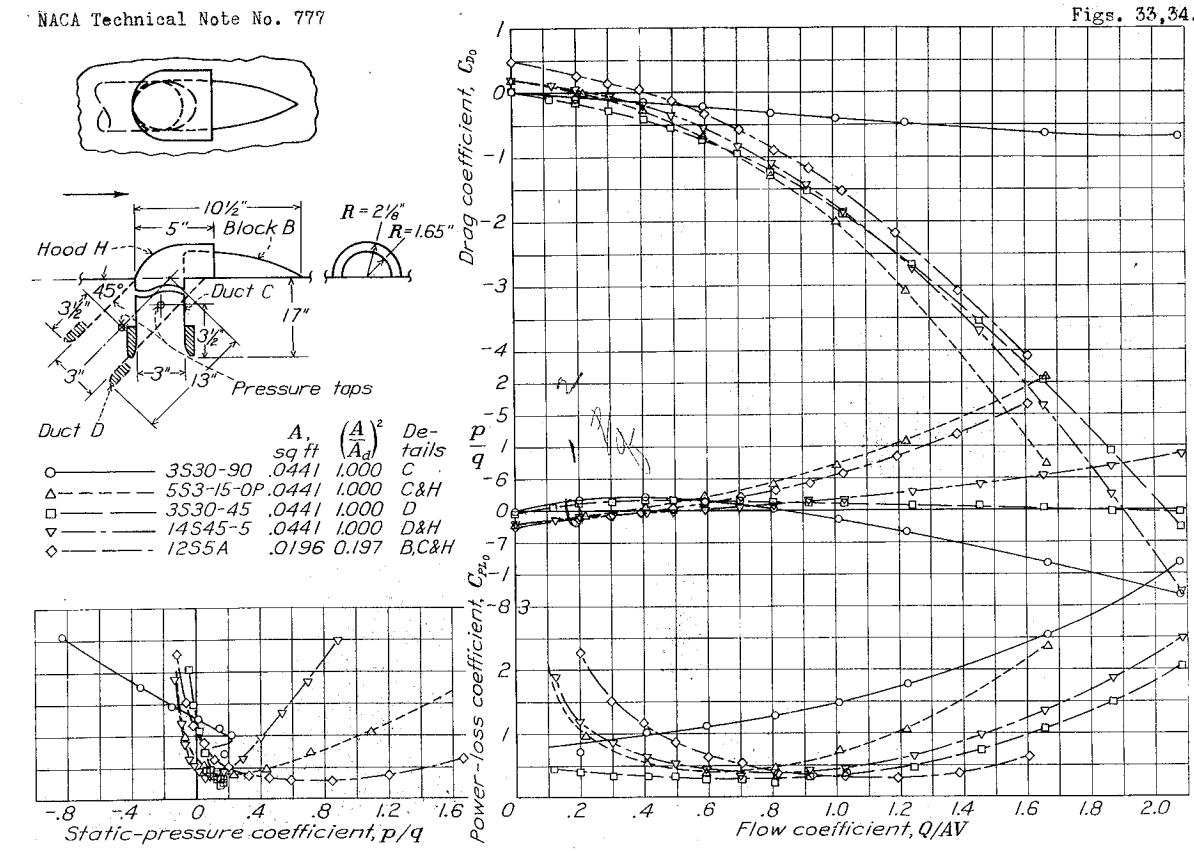

Figure 33.- Outlet characteristics of a hood over a circular duct in a flat plate.

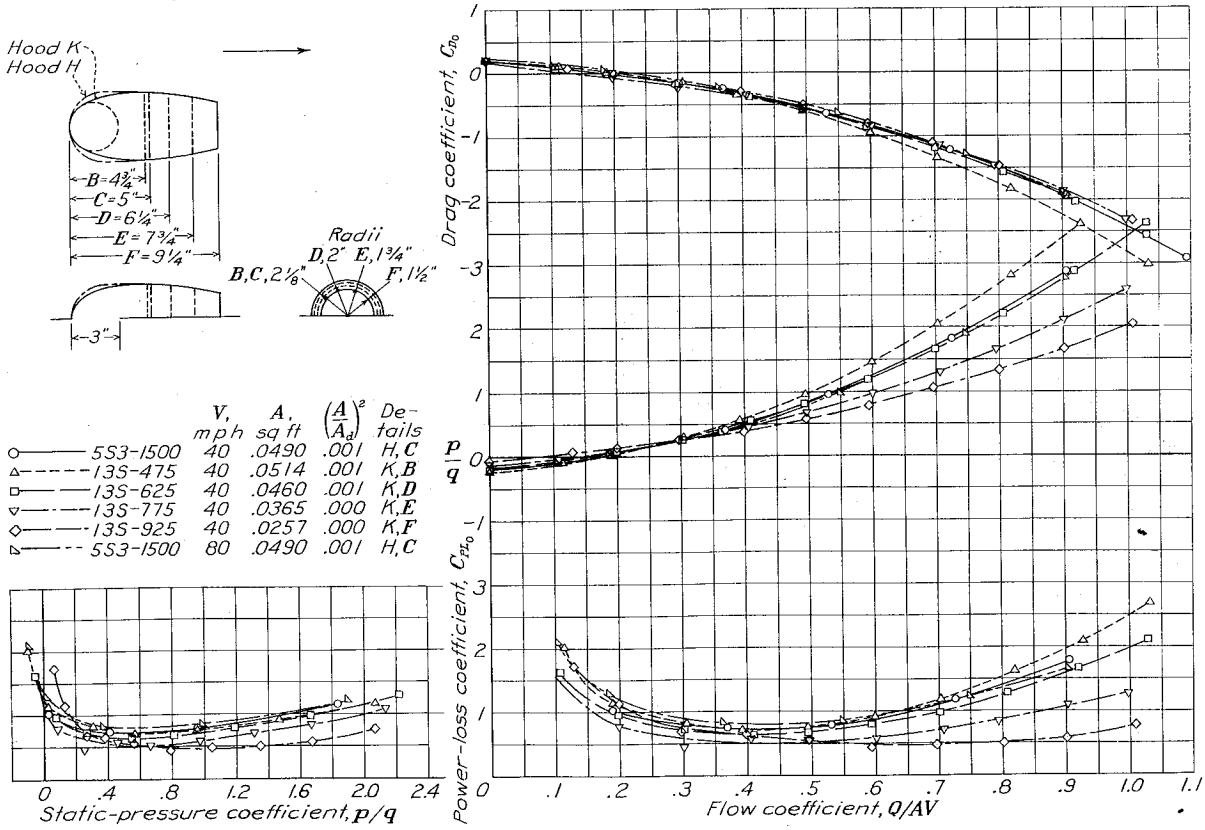

Figure 34.- Outlet characteristics of a hood over a circular hole in a flat plate.

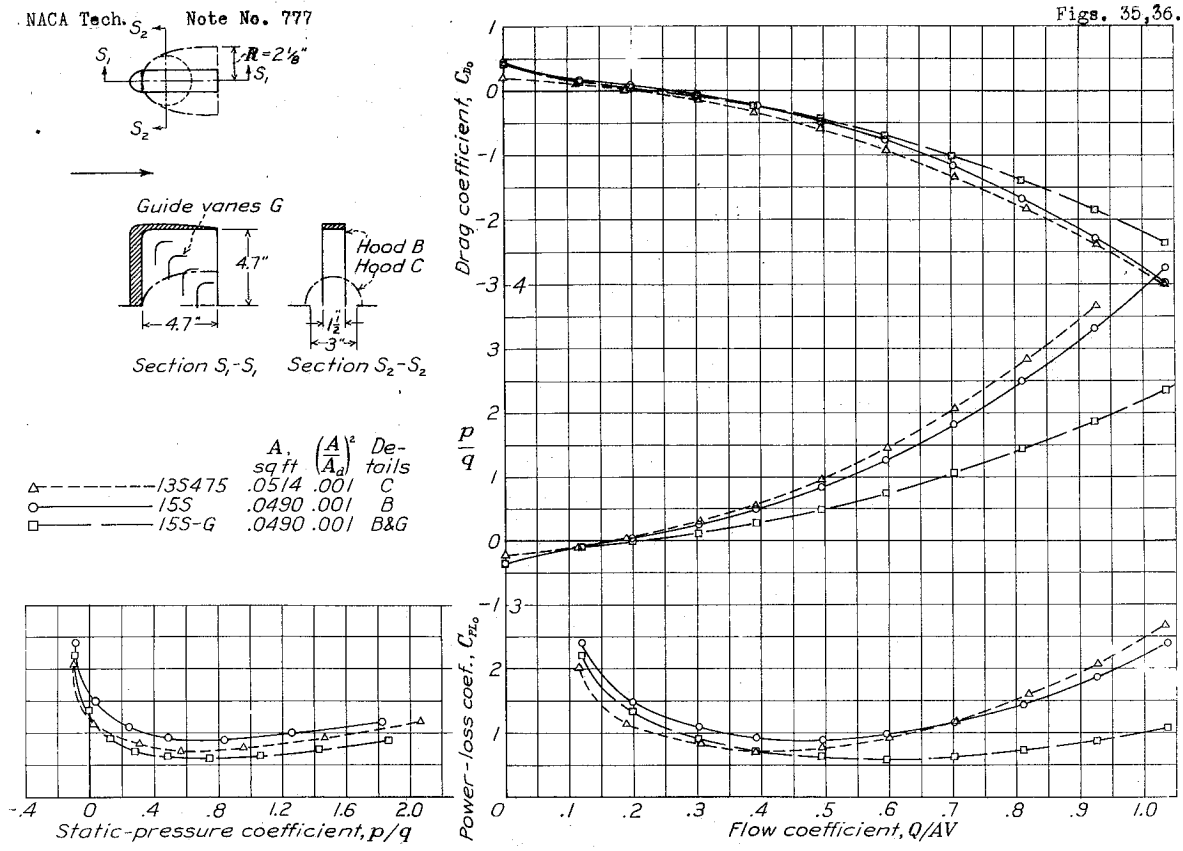

Figure 35.- Outlet characteristics of a high, thin hood over a hole in a flat plate.

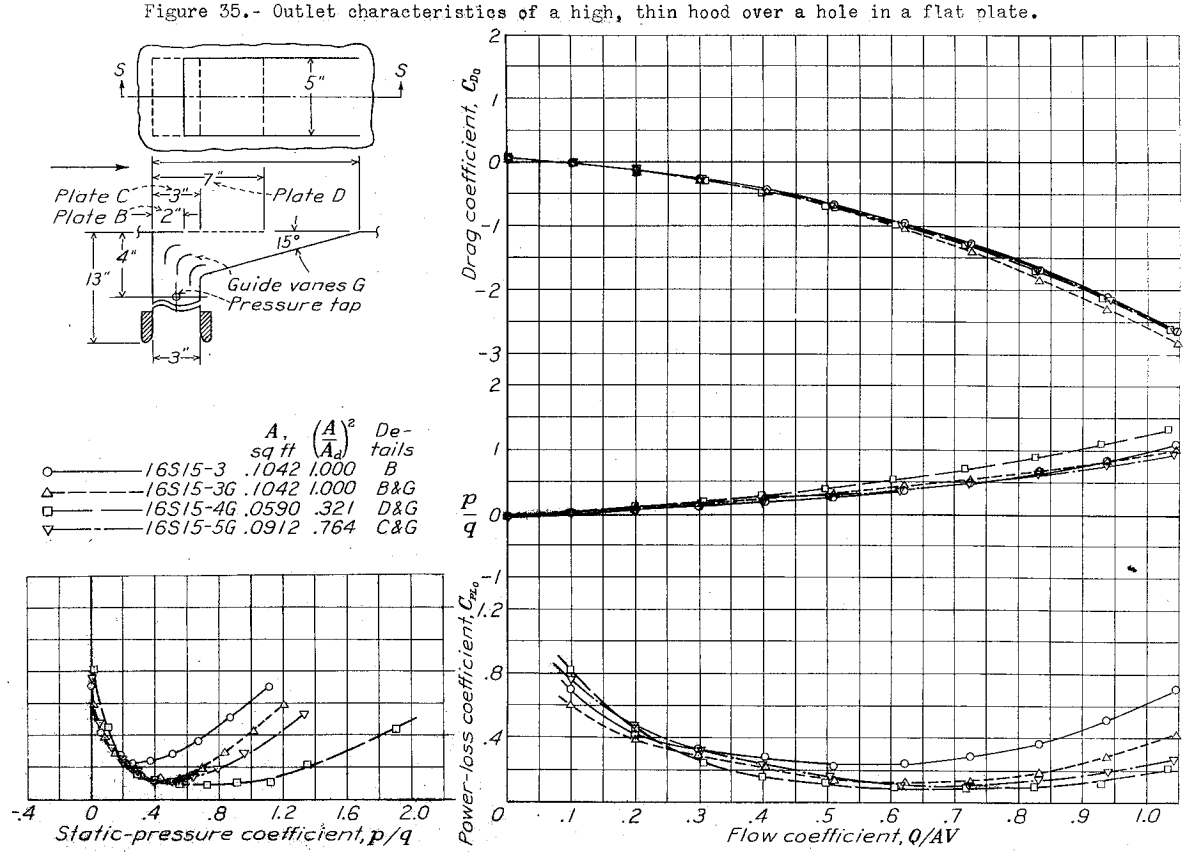

Figure 36.- Outlet characteristics of a flush recessed opening in a flat plate.

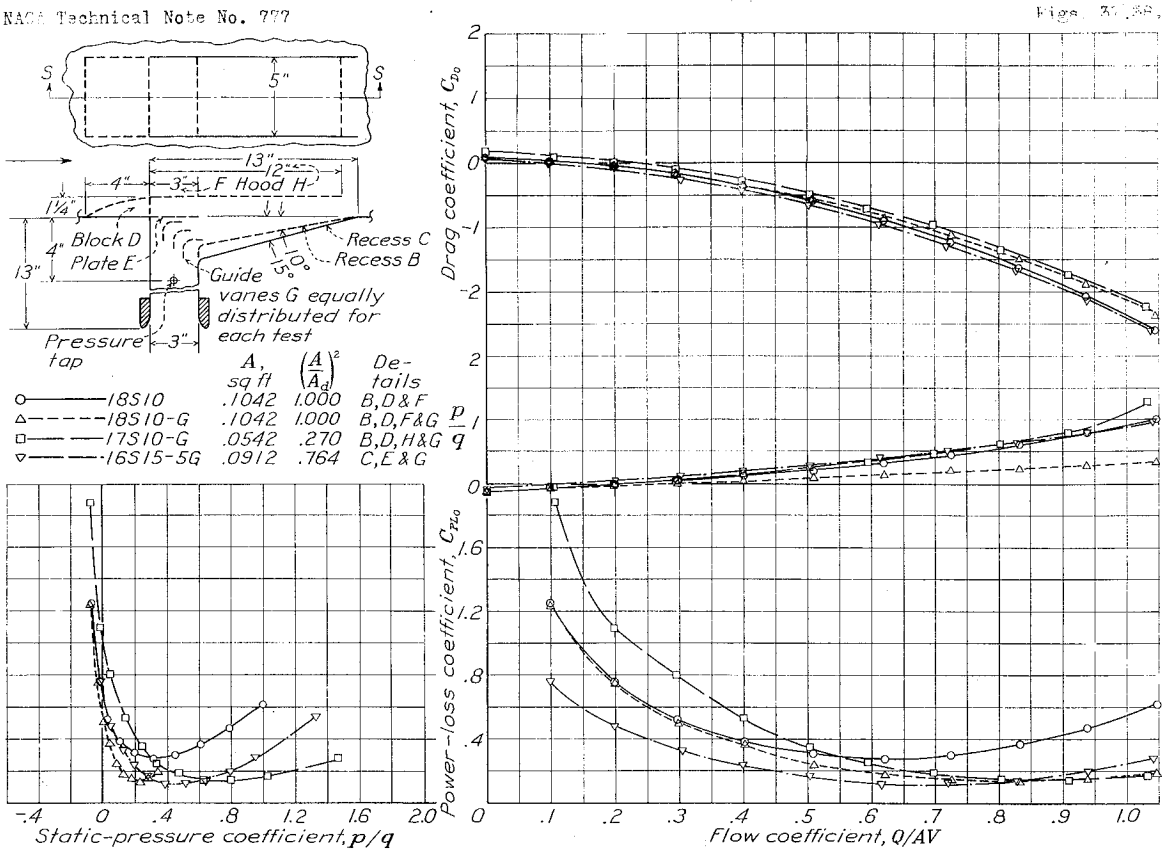

Figure 37.- Outlet characteristics of a recessed opening with a projecting hood in a flat plate.

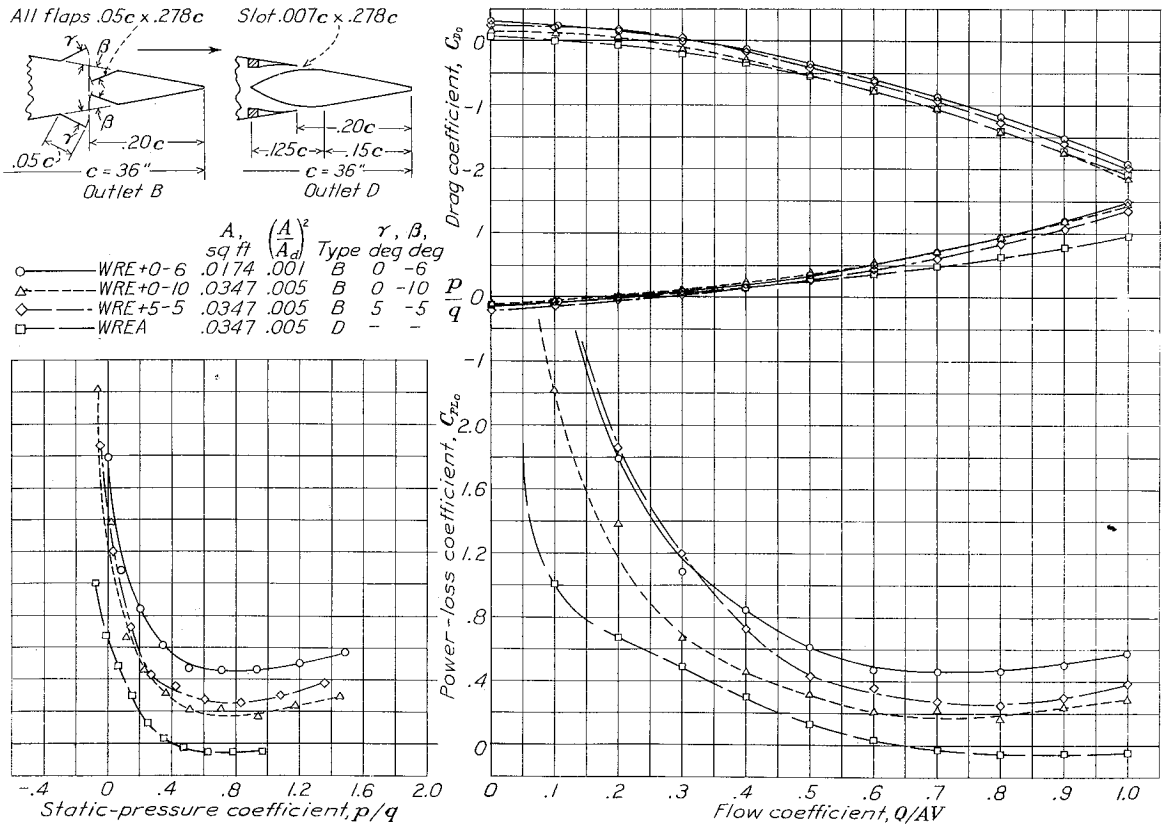

Figure 38.- Outlet characteristics of an adjustable-flap and faired openings at 0.20c in an NACA 0012 wing

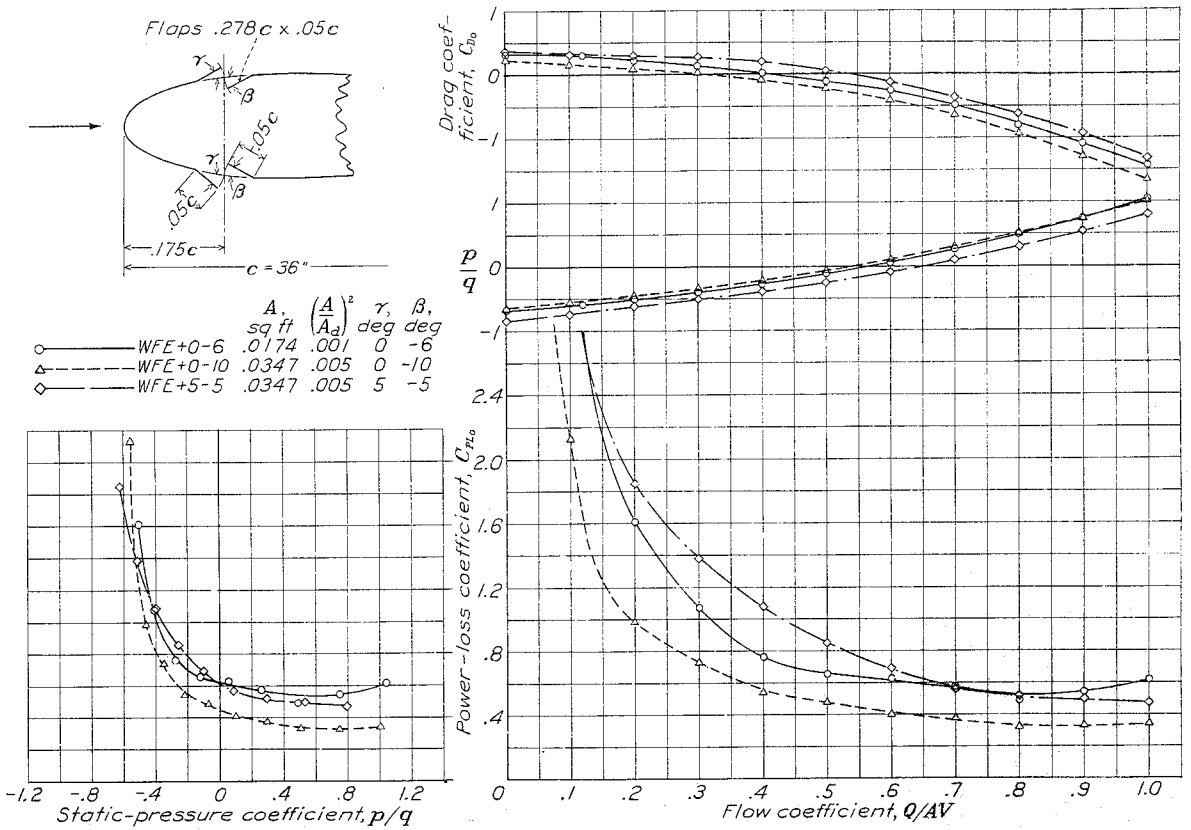

Figure 39.- Outlet characteristics of an adjustable-flap opening at 0.175c in an NACA 0018 wing.